Journal of Non-Crystalline Solids 619 (2023) 122581

Contents lists available at ScienceDirect

Journal of Non-Crystalline Solids

journal homepage: www.elsevier.com/locate/jnoncrysol

Review

Glass and glass ceramic electrodes and solid electrolyte materials for lithium ion batteries: A review

Zihan Wang [a,b,d], Shao-hua Luo [a,b,d,*], Xian Zhang [a,b,d], Song Guo [a,b,d], Pengwei Li [a,c], Shengxue Yan [a,b,d]

[a] School of Materials Science and Engineering, Northeastern University, Shenyang 110819, China
[b] School of Resources and Materials, Northeastern University at Qinhuangdao, Qinhuangdao 066004, China
[c] Department of Chemistry and Bioscience, Aalborg University, 9220 Aalborg, Denmark
[d] Key Laboratory of Dielectric and Electrolyte Functional Material Hebei Province, Qinhuangdao, China

ARTICLE INFO

Keywords:
Lithium-ion battery
Anode
Glass
Glass ceramic
Metal-organic framework (MOF)

ABSTRACT

Due to its distinct network structure, lack of a grain boundary, and isotropic qualities, glass has been the subject of extensive research. Lithium ion batteries can have their capacity and safety increased by using glassy electrode and electrolyte materials. We discuss the properties and uses of several types of glass and glass ceramic as anodes, including tin oxide glass, vanadium oxide glass, and so on. Metal-organic framework (MOF) materials are also investigated as a new generation of high-performance anode materials. We present the usage of glassy MOF materials to overcome MOF material volume change during charge and discharge, as well as the order and disorder transition of certain MOF materials during charge and discharge. The use of vanadium-based glass as a cathode material is also discussed. These materials have the potential to be employed as electrode materials in the next generation of lithium- ion batteries. In addition, the application of glass, especially sulfide glass, as an all-solid-state battery electrolyte and the effect of mixed anion effect on improving the conductivity of solid electrolyte were introduced.

1. Introduction

The development of more sustainable energy storage and conversion technologies is essential due to the gradual depletion of fossil fuels and the resultant environmental harm [1]. One of the main energy storage technologies, lithium ion batteries (LIBs), currently dominate the commercial sector [2]. The evolution of electronic devices powered by lithium-ion batteries has an impact on every aspect of daily life. Lithium-ion batteries have high energy density ($250 Whkg^{-1}$) and enough cycle life, which makes them not only widely used in portable electronic devices but also provide huge market shares for energy storage devices [3]. New generation batteries must meet two fundamental requirements: high energy density and safety [4]. The growing demand for lithium-ion batteries needs the development of novel electrode and electrolyte materials. At present, the development of lithium ion battery materials is mainly focused on two aspects: (i)Creating solid electrolytes to improve safety; (ii)Developing innovative high-capacity electrode materials to improve energy density [5]. New glass materials have received a lot of attention recently in the field of energy storage, particularly for use as electrodes and solid electrolytes in all-solid-state batteries (SSBs). The study of glass electrode and electrolyte materials has aroused widespread interest (Fig. 1).

Many attempts have been made to identify acceptable anode materials with high capacity and good cycle performance. Graphite is now the most often used commercial anode material due to its extended cycle life and inexpensive cost. However, because graphite can only intercalate one lithium ion with six carbon atoms, the comparable reversible capacity is only 372 $mAhg^{-1}$ [6,7], which prevents its use in large commercial applications. Although the capacity of lithium metal is as high as $3860 mAg^{-1}$ and is regarded as a potential anode [8], it involves safety concerns with dendritic development, which might result in a short circuit between electrodes. In comparison to crystalline anode materials, glass anode has received interest as an alternative for rechargeable lithium-ion batteries due to its distinctive structure, such as non-grain boundary, randomly dispersed structural unit, and open network structure [9–10]. Lithium ions can be injected into the open network structure of the glass anode during the lithiation process. In addition, the infiltration path in glass materials contributes to the

* Corresponding author at: School of Resources and Materials, Northeastern University at Qinhuangdao, Qinhuangdao 066004, China.
E-mail address: tianyanglsh@163.com (S.-h. Luo).

https://doi.org/10.1016/j.jnoncrysol.2023.122581
Received 15 June 2023; Received in revised form 15 August 2023; Accepted 16 August 2023

diffusion of lithium ions, resulting in higher rate capability. Glass anodes are usually prepared into glass ceramics, and disordered/ordered transitions may occur during charge and discharge [11,12]. Open glass networks, as opposed to nanocrystals, which serve as active sites for electrochemical conversion and alloying processes, can withstand volume change and stress caused by lithium injection during cycling. When compared to pure glass anode material, glass ceramics anode material provides greater electrochemical performance [13–16]. Metal-organic frameworks (MOFs), a novel type of porous materials composed of metal nodes and organic ligands, have gained a lot of interest due to their fascinating properties [17,18]. Because of their large specific surface area, customizable porous structure, many reaction sites, and high redox activity, MOFs are regarded to be potential energy storage materials [19–21]. However, certain research has revealed that MOFs typically display low conductivity, poor structural stability, and limited rate capacity when employed as anodes for lithium ion batteries, which ultimately restricts their practical applicability. Consequently, it is suggested that ordered/disordered engineering be used to enhance MOF anodes' electrochemical performance [22]. The amorphousization of polycrystalline MOF can be accomplished in a variety of additional ways, such as mechanical synthesis, mechanical ball milling, heat treatment, and pressure treatment, in addition to the ordered and chaotic transformation in the lithium/lithium removal process [23]. In addition to mechanically amorphous MOF, MOF glass is another disordered MOF that can be found. Certain zeolite imidazolate framework structural materials (ZIFs), a subclass of MOFs, can melt at high temperatures before decomposing and then quench into glass, a process known as melt quenching (MQ) MOF glass [24–26]. This new glass material family has fascinating structural and chemical properties, which can be used as the anode of lithium batteries and has good electrochemical performance.

Common lithium ion battery cathode materials are crystalline states such as $LiCoO_2$, $LiFePO_4$, ternary lithium, and so on [27]. Because of the existence of grain boundaries, the crystal cathode material lowers the efficiency of lithium-ion transport. Because of the discovery and development of new cathode materials for lithium-ion batteries, as well as the research of quick ion conductors, the exploration of oxide glass as a cathode material for lithium-ion batteries has rapidly garnered interest. The glass electrode material differs significantly in size from the crystalline electrode material and exhibits a very disordered and stable three-dimensional network structure. Large-diameter cations in the glass-formed network are hindered in the migration process, allowing only small-diameter lithium ions to pass through. The network structure's lattice unit prevents the lithium ions from being bound during the migration phase, considerably increasing their efficiency and allowing the material to surpass its intrinsic specific capacity [28]. Because vanadium has numerous oxidation states, vanadate glass has been extensively researched among several glass cathode materials. Binary glass vanadium-based materials V_2O_5-P_2O_5 [29,30] and TeO_2-V_2O_5 [31] have, as far as we are aware, been investigated as electrode materials for a very long period. By doping metal oxides, vanadate glass cathode electrochemical performance can be enhanced. The "mixed network forming agent effect" will be created when the network forming agent is introduced, improving the electrochemical performance. As effective glass forming agents, phosphate, borate, silicate, and other polyanion combinations are employed [32–35]. Vanadium-based ternary and quaternary glass cathode materials have also been the subject of several investigations.

The traditional LIB uses a flammable organic liquid electrolyte, which has leakage and fire risks. An inorganic solid electrolyte can be used in place of a liquid electrolyte to increase the safety and dependability of batteries [36,37]. The safety of a solid electrolyte solid-state lithium battery has substantially improved, and the use of a metal lithium anode is now possible. The next generation of high energy

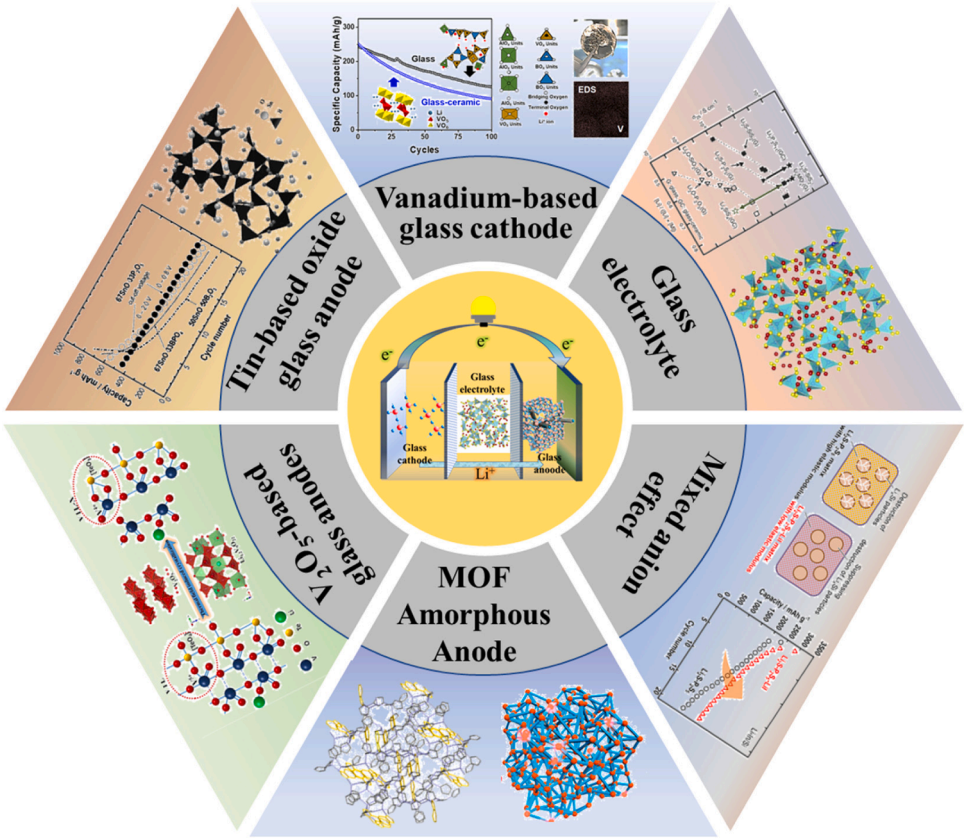

Fig. 1. Glass electrode and electrolyte in lithium ion battery.

density, high cycle performance batteries are expected to be completely solid state batteries [38–40]. In batteries, the inorganic solid electrolyte is employed because it not only provides a large electrochemical stability window, but also improves safety, durability, and energy density, and simplifies battery design. There has been a lot of discussion about employing inorganic solid electrolytes instead of organic liquid electrolytes. The sulfide-based solid electrolyte has emerged as aromising candidate electrolyte due to its higher ionic conductivity and bigger electrochemical window than oxide electrolyte. Sulfide-based solid electrolytes are generated by sulfur ions substituting oxygen ions in oxide-based solid electrolytes [41–44]. Because sulfur binds to lithium ions with less force than oxygen does, there may be more lithium ions that are free to move because sulfur has a lower electronegativity than oxygen. The sulfur ion has a radius that is larger than the oxygen ions. Sulfide solid electrolytes can produce a sizable migration channel for lithium ions to help in their movement. As a result, the sulfide solid electrolyte displays a high ionic conductivity at room temperature, which is around 10^{-3}–10^{-4} Scm^{-1} [45–47]. Glass has long been investigated as a solid electrolyte. Although sulfide glass has stronger mechanical properties than liquid electrolytes and is simple to produce at low temperatures, it has poor water stability. Oxysulfide glasses have been investigated as a basis for a middle ground for a workable compromise, although only glass electrolytes have been added thus far [48–50].

In this review, we introduce the properties of Tin-based oxide glass anodes including SnO-P_2O_5 glass [51–55], SnO-B_2O_3 glass [56–58], Vanadium-based oxide glass including V_2O_5-P_2O_5 glass [59–64], TeO_2-V_2O_5 glass [65–69] and other oxide glass [70,71–73] as anode materials for lithium ion batteries. The advantages of molten quenched glass ZIF-62 [23,25,74,75] as anode material and the ordered disorder transition of MOF anode material during charge and discharge are introduced [22,76]. The use of binary and multicomponent vanadium-based glasses as cathode materials are examined, as well as the influence of a mixed glass network forming agent on the electrochemical parameters of vanadium-based glasses [32–35]. In addition, the advantages and application prospects of glass, especially sulfide glass [77–83], as high-performance solid electrolyte materials, and the use of mixed anion effect to improve the conductivity of glass electrolyte are introduced [80,82,84,85]. We put forward opinions and suggestions on the future development of new generation anode materials and all-solid-state battery electrolyte materials.

2. Glass anode

Battery anode materials require high energy density and good cycle stability. At present, The two basic requirements in addition to graphite materials, the cycle stability and safety performance of other types of anode materials are still not satisfactory, but the theoretical energy density of graphite materials is only 372mAhg^{-1} [86]. Compared with the crystal anode materials studied more in the past, the glass anode has attracted much attention due to its advantages of easy preparation, unique open network structure with infiltration channel, no grain boundary, flexible composition, and easy adjustment of crystal content. Table 1 shows some glass materials that can be used as anodes and their capacity. Glassy materials do not have regular lattice structures and crystal boundaries like crystalline materials [51,55,87]. This open network structure can form lithium-ion deintercalation channels, which are conducive to lithium-ion diffusion and transmission; so that the battery can obtain stable cycle performance and rate performance [10,68,70]. In addition, regulating the glass network structure to improve the conductivity and ion transport efficiency of the glass to achieve better lithium storage performance can be achieved by controlling the component ratio, and cooling time, or improving the heat treatment process, doping heterogeneous elements, crystallization and other methods [88,89].

Table 1
Some glass anode synthesis methods and Capacity.

Anode	Physical condition	Method of combining	Capacity	Refs.
67SnO-33P_2O_5	Glass	Melting quench	400 mAhg^{-1} 0–0.8 V 20 cycles	[51]
72SnO-28P_2O_5+48AlN	Glass-ceramic	Melting quench	Heat treatment at 500 °C 750 mAhg^{-1}, 550 °C 470 mAhg^{-1}	[52]
72SnO-28P_2O_5	Glass	Melting quench	550 and 160 mAhg^{-1} at room temperature and −20 °C	[90]
SnB_2O_4	Glass-ceramic	Melting quench	540 mAhg^{-1} 0–0.8 V 40 cycles	[91]
50SnO-50B_2O_3	Glass	Mechanical milling	184 mAhg^{-1} 20 cycles	[56]
75V_2O_5–25P_2O_5+GNP	Glass	Melting quench	447mAhg^{-1} 100 cycles	[92]
80V_2O_5–20P_2O_5	Glass	Melting quench	337mAhg^{-1} 600 cycles	[87]
40TeO_2–60V_2O_5	Glass	Melting quench	121mAhg^{-1} 5000 cycles	[66]
77$SiO_2$23GeO_2	Glass-ceramic	Melting quench	520mAhg^{-1} 100 cycles	[93]
50Fe_2O_3–50P_2O_5	Glass-ceramic	Melting quenching (heat treatment in reducing atmosphere)	373mAhg^{-1} 1000cycles	[72]

2.1. Tin-based oxide glass anode

Tin oxides include substances like stannous oxide, stannic oxide, and mixtures of the two. In comparison to the 372mAhg^{-1} theoretical capacity of carbon, tin oxide has a specific capacity of almost 500mAhg^{-1}. The tin oxide anode's first irreversible capacity loss, which is mostly related to the reaction process, approaches 50% [94–96]. Li_2O and SEI films are generated during the first charge and discharge process. Another problem is the large volume change of materials during lithium intercalation and deintercalation (SnO_2, Sn, Li density are 6.99 gcm^{-3}, 7.29 gcm^{-3}, 2.56 gcm^{-3}, Large volume change of materials before and after charge and discharge) easily lead to electrode pulverization or agglomeration, resulting in electrode specific capacity attenuation and cycle performance decline [95,97–99].

The two main lithium storage mechanisms of tin-based oxides are ionic and alloy-type. The ion-type lithium storage mechanism is as follows.

$$xLi + SnM_xO_y \leftrightarrow LixSnM_xO_y \quad (1)$$

Alloy production is a different reaction mechanism. Tin then reacts with lithium to create alloys when Li reacts with oxides to produce Li_2O and tin metal:

$$2Li + SnM_xO_y \rightarrow Li_2O + Sn + \frac{1}{2} M_xO_y \quad (2)$$

$$4.4Li + Sn + 2Li_2O + \frac{1}{2}M_xO_y \leftrightarrow Li_{4.4}Sn + 2Li_2O + \frac{1}{2}M_xO_y \quad (3)$$

Nearly all of the experimental phenomena support the alloy-type lithium storing mechanism. Sn particles were formed after charging and discharging of 72SnO·28P_2O_5 glass anode, as shown in Fig. 2(c,d). According to the alloy-type deintercalation mechanism, the creation of Li_2O in the first stage and the breakdown or condensation of Sn oxides with organic electrolyte in the second step result in the initial irreversible capacity [100–102]. The reversible capacity results from the

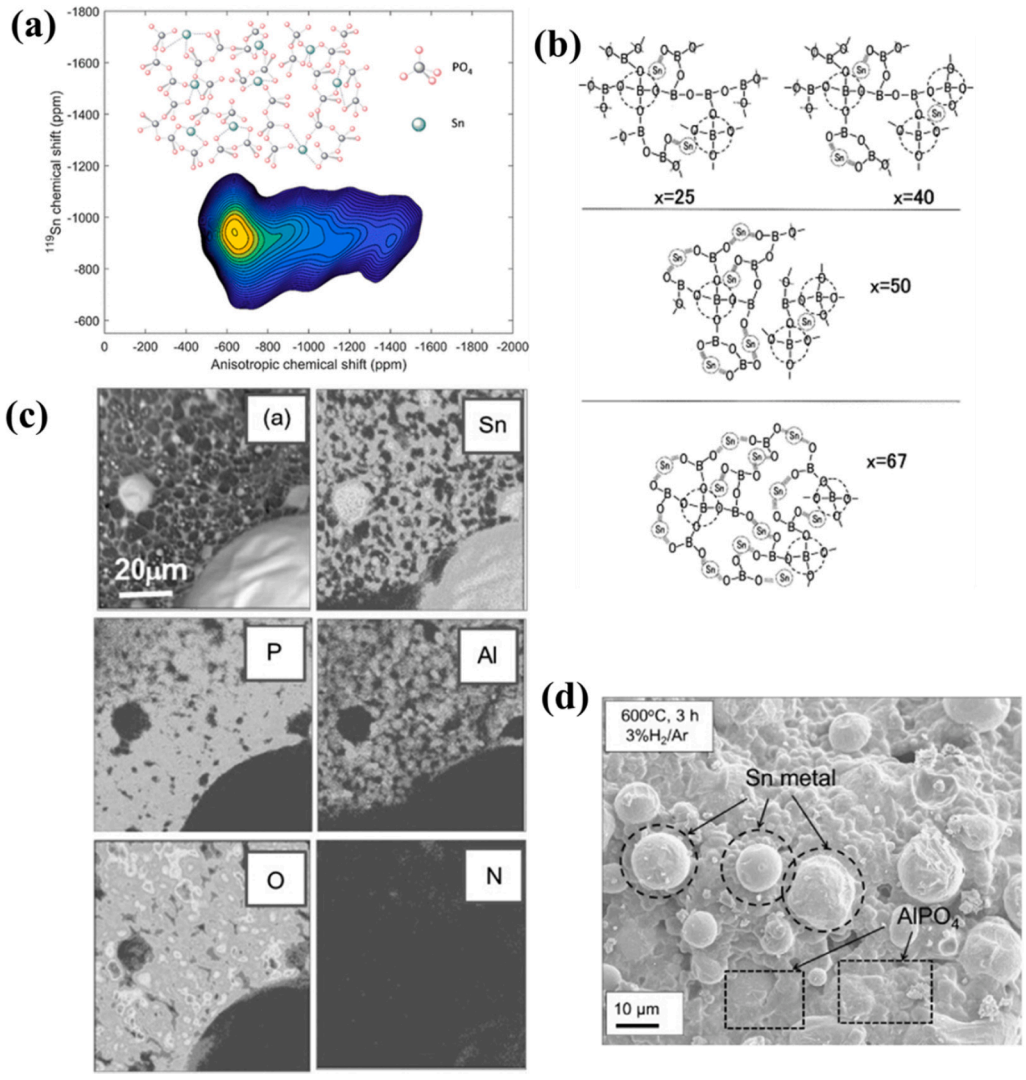

Fig. 2. (a) The network structure of binary SnO-P_2O_5 glass is demonstrated by two dimensional ^{119}Sn and ^{31}P NMR spectra. Reproduced with permission from Ref. [55] Copyright 2018 American Chemical Society. (b) Structural models of the $xSnO{\cdot}(100-x)B_2O_3$ glasses. Reproduced with permission from Ref. [57] Copyright 2002 Elsevier. (c) and (d) EPMA and SEM photographs for $72SnO \cdot 28P_2O_5$ glass anode containing Sn particles. Reproduced with permission from Ref. [52] Copyright 2014 Elsevier.

reversible reaction of Sn and Li creating alloy. Before the substitution and alloying events, the organic electrolyte decomposes on the surface of the particles, creating an amorphous passivation coating. The passive film is constructed of alkyl Li and Li_2CO_3 and is several nanometers thick. ($ROCO_2Li$). The substitution reaction produces fine Sn nanoparticles that are widely disseminated in lithium oxide. Nanometer sizes are also produced via the alloying reaction for Li and Sn [103,104]. The presence of nano-sized Li particles in the reaction products explains why Sn oxides have such a high capacity as anode materials. Because irreversible Li_2O is created in the first step, the first charge-discharge efficiency is quite poor. The separated metal Sn and Li_2O phases were identified by XRD analysis, but not the homogeneous $LixSnO_2$ phase. Electron paramagnetic resonance spectroscopy and XPS analysis both show the existence of Li atoms in Sn oxides. Sn oxides represented by SnO were analyzed using XRD, Raman, and high-resolution electron microscopy to show the alloy-type deintercalation mechanism of Sn oxides. Although tin oxide can also be used as a cathode material, it is difficult for glassy tin oxide to undergo intercalation reactions like crystal cathode materials, so most tin-based oxide glasses are used as anodes.

The study of tin-based composite oxide (TCO) began in Fuji, Japan. Researchers became interested in amorphous tin-based composite oxides after learning that they possessed a high reversible specific capacity and a long cycle life [105]. As a result, a great deal of research on this subject has been published. Tin-based composite oxides have the potential to partially address the issues with Sn oxide anode materials that have a high irreversible capacity for the initial charge and discharge as well as poor cycle performance. The process entails heating Sn oxides after adding some metal or non-metallic oxides, such as B, Al, Si, Ge, P, Ti, Mn, and other oxide elements. The amorphous structure of the tin-based composite oxide is combined with additional oxides to create an amorphous vitreous body. The usual formula for it is th, therefore, M_xO_y, where M denotes a collection of metal or non-metal elements (1–3 kinds) that make up the vitreous body, frequently B, P, Al, and other oxides [55,106–109]. Tin-based composite oxides are composed of Sn-O bonds in the active center and a random grid structure surrounding it, so the effective lithium storage capacity is proportional to the active center. The common structure of SnO-P_2O_5 and SnO-B_2O_3 which can be used as anode is shown in Fig. 2(a,b). Tin-based composite oxide has a reversible specific capacity of 600mAhg^{-1} and the volume-specific capacity exceeds 2200mAhcm^{-3}, which is roughly twice the capacity of carbon anode material [96].

2.1.1. *SnO-P_2O_5*

Idota's [105] team pioneered the use of glass as an anode for lithium-ion batteries as early as 1997. The traditional flow argon melting quenching method was used to create $Sn_{1.0}B_{0.56}P_{0.40}Al_{0.42}O_{3.6}$ (TCO-1) glass. TCO anode has a reversible lithium adsorption capacity that is more than 50% greater than carbon when combined with lithium cobalt cathode. Measurements of lithium-7 nuclear magnetic resonance

show that lithium maintains a high ion state when charged, with 8 mol of lithium ions per mole of TCO. Akitoshi Hayashi et al. [51] also prepared a simple binary SnO-P_2O_5 glass by melting quenching method and studied its electrochemical properties. Raman spectroscopy (Fig. 3a) shows that with the increase of SnO content, the phosphate network is depolymerized, and the discharge capacity of the battery is roughly increasing (Fig. 3b). The battery using 67SnO/33P_2O_5 glass as anode has good cycle performance, with a capacity of more than 400mAhg^{-1} in the voltage range of 0–2.0 V and 20 cycles.

A glassy SnO-P_2O_5 anode material was developed by Hideo Yamauchi and colleagues [90]. (GSPO). In comparison to the half-cell with a graphite anode, the half-cell with a GSPO anode had a reconstruction capacity of 550 and 160 mAhg^{-1} at room temperature and −20 °C, respectively. No dendritic deposition was seen even at −20 °C. Inhibiting volume change during the charge-discharge cycle is possible with the structure of GSPO, which also has strong low-temperature performance and high-temperature endurance.

When SnO-P_2O_5 glass is used as an anode for lithium-ion batteries, the reaction type of anode charging/discharging is generally alloy type: first, lithium oxide is formed, and then lithium oxide and tin generate alloy. The reaction to generate lithium oxide is irreversible, resulting in large capacity loss during the first charge/discharge. Kondo et al. [52] proposed utilizing aluminum nitride powder as a reducing agent and SnO-P_2O_5 glass powder as a non-electrochemical reaction for the creation of Sn crystals in 72SnO-28P_2O_5 glass (Fig. 2c and d). Spherical Sn particles were generated after heat treating the glass and AlN (72SnO-28P_2O_5+48AlN) with 3%H_2/Ar mixed powder, significantly lowering the irreversible capacity in the battery performance. The sample with Sn particles acquired by heat treatment at 550 °C has a little lower charge capacity 470mAhg^{-1} than the sample produced by an electrochemical reaction. (550 mAhg^{-1}). The creation of new anode materials has a high potential thanks to SnO-P_2O_5 glass with Sn particles.

2.1.2. SnO-B_2O_3

SnO-B_2O_3 glass is an important low melting point glass, and B_2O_3 has a strong glass-forming tendency [110]. This allows more SnO to exist in the SnO-B_2O_3system, which increases the capacity. Another promising glass anode for lithium ion batteries that have received a lot of attention is SnO-B_2O_3 glass. As early as 2003, Gejke et al. [91] studied the thermal stability and cycling performance of SnB_2O_4 glass. The effects of potential range and electrolyte composition on cycle stability were studied. The results show that the capacity of the material is about 530 mAhg^{-1}, and the cycle is at least 40 times. The potential range is influenced by cycle performance, and a steady cycle can be guaranteed by a 0.8 V charging limit. The discharge potential is not limited and the stability is good when cycling between 0.2 V and 0.01 V. With only a tiny change in capacity between electrolytes, this material can be employed in a variety of electrolyte systems without degrading cycle performance, which is another significant benefit. Additionally, the glass is more thermally stable than graphite anodes that use $LiPF_6$ or LiTFSI salts in electrolytes.

In addition to the melting quenching method, the amorphous electrode can also be prepared by mechanical ball milling. A. Hayashi et al. [56] prepared SnO· (100−x) B_2O_3 ($0 \leq x \leq 80$) glass by mechanical milling. The glass's maximum Tg was 347 °C when SnO was 40mol%, and its reliance on glass composition for TG was comparable to that of the corresponding melt-spun glass. The discharge capacity and charge-discharge efficiency of the ground glass are greater than those of the melt-spun glass, particularly when $x = 67$ and 80. The SnO-B_2O_3 glass produced by mechanical milling contains BO_3 and BO_4 units, and the local structure surrounding the boron atom in the grinding glass is identical to that of the corresponding hardened glass, according to the MAS-NMR spectra. At a constant current density of 1.0 mAcm^{-2} and a cut-off voltage of 0~2.0 V, the electrochemical cell with ground glass was used to charge and discharge 20 cycles. The glass with $x = 50$, 67, and 80 had high charging capacity (>1100 mAhg^{-1}) and discharge capacity (>700 mAhg^{-1}). The battery with 50SnO-50B_2O_3 glass has a discharge capacity of 184 mAhg^{-1} and a charge-discharge efficiency of 100% after 20 cycles. Experiments show that mechanically milled

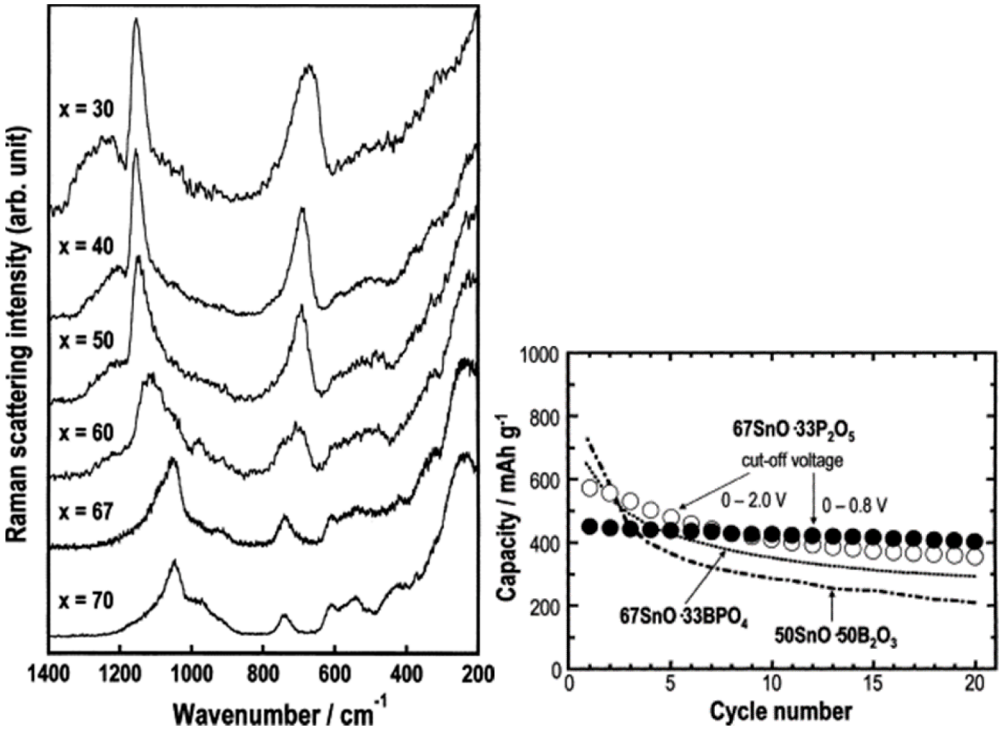

Fig. 3. (a)Raman spectra of the xSnO·(100−x)P_2O_5 glasses,(b) Cycle performance for the cells using the 67SnO·33P_2O_5 (mol%) glass under the two different cut-off voltage conditions of 0–2.0 and 0–0.8 V Cyclability for the cells with 50SnO·50B_2O_3 (mol%) and 67SnO·33BPO_4 (mol%) glasses is also shown for comparison. Reproduced with permission from Ref. [51] Copyright 2004 Elsevier.

SnO-B_2O_3 glass and quenched glass can be used as anode materials for lithium secondary batteries.

2.2. Vanadium-based glass anodes

The properties of vanadium-based materials, which are anticipated to become a new generation of electrode materials, include variable multi-electron reaction, rich vanadium-oxygen coordination structure, large inter-layer domain layered structure, and wide three-dimensional skeleton structure in tunnel space [111]. Because V_2O_5 glass may be used as both the cathode and anode of lithium-ion batteries, it has received much research as a glass electrode. Glass anodes made of V_2O_5 have been thoroughly investigated. glass electrodes made of V_2O_5, such as V_2O_5-TeO_2. [112], V_2O_5-P_2O_5, for high energy density LiBs has attracted considerable attention Since V_2O_5 has a layered structure that is conducive to the insertion reaction with $Li^+$and simultaneously exhibits ionic and electronic conductivities. The reaction of vanadium-based glass as anode material during charge and discharge is similar to that of tin-based glass, The irreversible capacity is due to the first step to generate Li_2O, and the reversible capacity is caused by alloying of V and Li.

2.2.1. V_2O_5-P_2O_5

In V_2O_5-P_2O_5 glass, the basic structural units of vanadium and phosphorus are VO_5 triangular pyramid, VO_4 tetrahedron, and PO_4 tetrahedron. These structural units form glass mesh structures according to the four-tooth model [113,114]. Therefore, the VP glass structure forms a layered three-dimensional network structure, which provides an open channel for lithium ion migration and limits the low-valent vanadium ions in the frame structure.

As early as 1985 Y. Sakurai and J. Yama [115] made V_2O_5-P_2O_5 glass as lithium battery cathode material. Sakurai and Yamaki [116] prepared $75V_2O_5$–$25P_2O_5$ glass graphite composite (GNP) as the anode material with excellent application performance for lithium ion batteries and compared the electrochemical properties of the original $75V_2O_5$–$25P_2O_5$ glass and graphene nanosheets modified $75V_2O_5$–$25P_2O_5$. In comparison to $75V_2O_5$–$25P_2O_5$, which has a first discharge capacity of 1409mAhg^{-1} and a reversible discharge capacity of 693mAhg^{-1} at 200 mAg-1 current density, the glass anode of $75V_2O_5$–$25P_2O_5$ has a first discharge capacity of 1644mAhg^{-1} and a reversible discharge capacity of 812mAhg^{-1}. After 100 cycles, the GNP modified $75V_2O_5$–$25P_2O_5$ has a capacity retention of 55% and a discharge capacity of 447mAhg^{-1}. It is found that the graphene-modified sample becomes more stable after the 20th cycle and keeps 98% of its capacity after 100 cycles. To enhance the performance of amorphous vanadium-based lithium battery anode

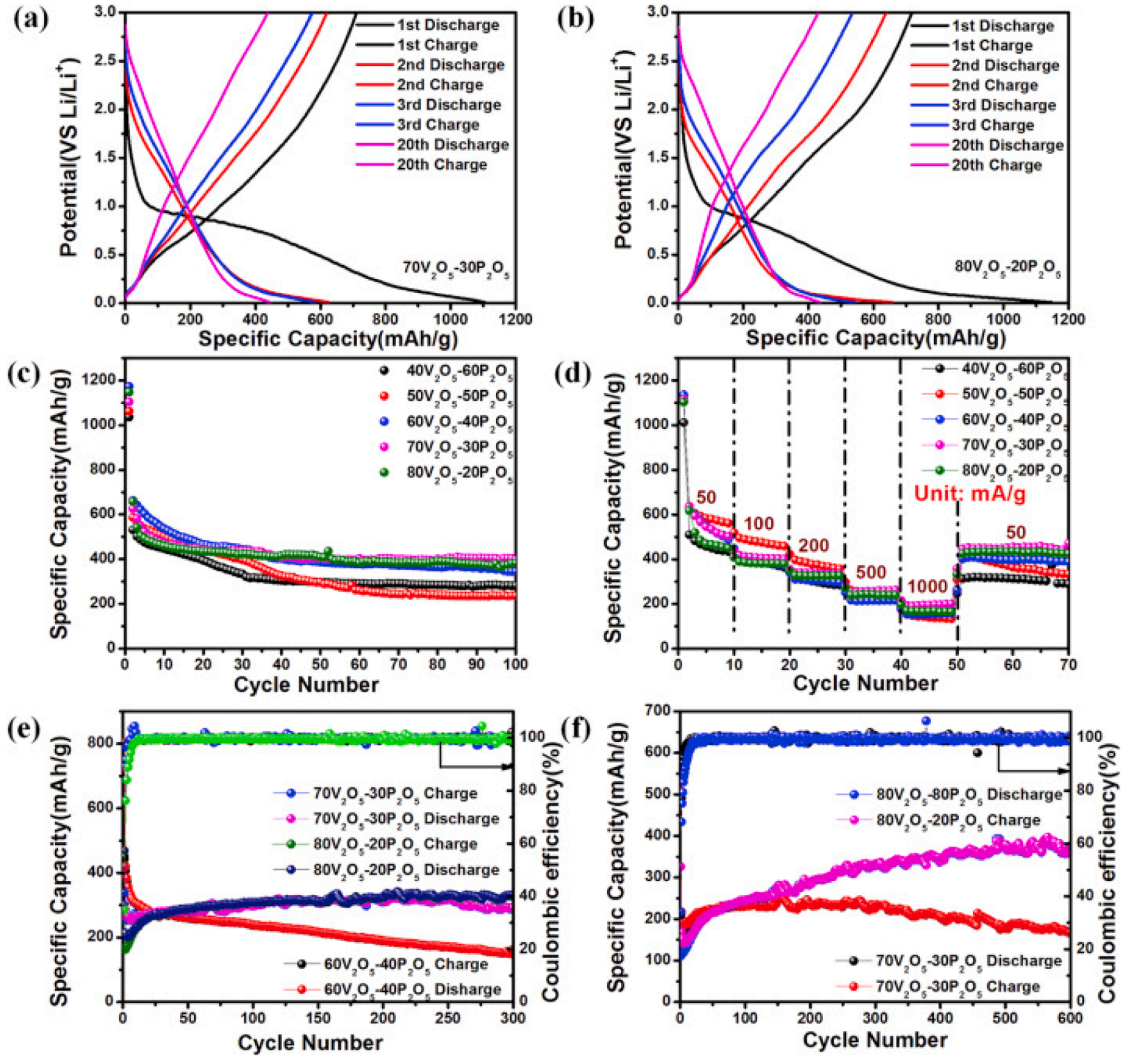

Fig. 4. The discharge-charge curves of $70V_2O_5$–$30P_2O_5$ (a) and $80V_2O_5$–$20P_2O_5$ (b) from 0.01 to 3 V at 50 mA·g^{-1}; Cycle (c) and rate (d) performance of five samples at the current density of 50 mA·g^{-1}; Long-term cycle performance of $60V_2O_5$–$40P_2O_5$, $70V_2O_5$–$30P_2O_5$ and $80V_2O_5$–$20P_2O_5$ at 500 mA·g^{-1} (e), and of $70V_2O_5$–$30P_2O_5$ and $80V_2O_5$–$20P_2O_5$ at 1 A·g^{-1} (f). Reproduced with permission from Ref [87] Copyright 2019, Elsevier.

materials, Yu et al. [87] created a variety of vanadium phosphate glass and crystal materials using a straightforward melting quenching technique. The electrochemical results demonstrated that amorphous samples' cycle performance and rate performance were much superior to those of crystalline samples (Fig. 4). $80V_2O_5$–$20P_2O_5$ shows an irreversible capacity of 377 $mAhg^{-1}$ after 600 cycles at $1Ag^{-1}$ in situ XRD analysis results show that the amorphous structure can be retained during the insertion and extraction of lithium ions, which is beneficial to the long-term performance of lithium ions. The findings demonstrate that when vanadium concentration rises, lithium ion conductivity rises, and the diffusion coefficient falls, reducing the contribution of the diffusion control process. A straightforward and efficient method to raise the conductivity and lithium ion diffusion of vanadium phosphate glass electrodes is to raise the electrochemical performance of amorphous electrode materials.

2.2.2. TeO_2-V_2O_5

Tellurium-based glasses often exhibit better conductivity and dielectric constants when compared to other glass systems. During cycling, the vanadium telluride glass has the potential to produce nanocrystals, which greatly enhances the electrochemical attributes including capacity and cycle stability. In general, nanocrystals can be generated in glass by discharge/charge cycles if the composition of the glass is well designed. However, the microscopic cause of the creation of nanocrystals brought on by discharge or charge has not been identified [92]. The structure of V_2O_5-TeO_2-Li_2O after heat treatment was modeled. The conversion of $[VO_5]$ to $[VO_4]$ transformed the structure of $[TeO_4]$ into $[TeO_3]$. As shown in Fig. 5, the DFT model showed that the diffusion barrier of $V2O_5$-TeO_2-Li_2O decreased from 0.49 eV to 0.16 eV after heat treatment. After crystallization, the conductivity and specific capacity of the obtained electrode material are significantly improved.

Zhang [109] proposed and implemented a new strategy, namely disordered/ordered engineering, to develop a new anode material. To create disordered materials, many V_2O_5-TeO_2 (VT) liquids were glassed together. VT glass powder was then combined with binding agents and acetylene black to create the anode, which was then placed into lithium-ion batteries with lithium serving as the cathode and the proper electrolyte. The findings demonstrate that the disorder-order transition takes place when the battery is depleted or charged, partially transforming the VT glass into an ordered phase at the nanoscale. In the disordered matrix phase, ordered nanodomains are uniformly distributed, and as the discharge/charge cycle lengthens, so do their number and size. In the discharge/charging operation, the ordered nano-phase and disordered glass phase maintained a stable structure while enhancing ionic dynamics and electronic dynamics. The battery has excellent rate performance and good cycle stability.

In order to fully comprehend the electrochemical evolution during the cycle, including the redox reaction and the mechanism of nanocrystal creation, it is crucial to record the specifics of the evolution of short-range structures during the cycle. The secret to creating innovative glass components and high-performance lithium-ion battery pack electrodes is the local structure evolution of lithium-ion battery pack electrodes during cycling. This is also essential for developing a broad picture of the local structural alterations of amorphous electrodes during cycling in lithium-ion batteries. Jiang et al. [69] revealed the microstructure evolution of V_2O_5-TeO_2 glass during the anode discharge/charge cycle by solid-state nuclear magnetic resonance (NMR) technique (Fig. 6), thus clarifying its lithium ion mechanism. They found that the 3D network structure of the prepared glass was completely broken into negatively charged substances during cycling, such as $[PO_4]^{3-}$, $[VO_4]^{3-}$, $[V_2O_7]^{4-}$, $[TeO_3]^{2-}$ and $[Te_2O_5]^{2-}$, which bind to Li^+ ions. Driven by this type of species formation and migration, Li_2Te nanocrystals are formed by inserting Li^+ ions in the discharge/charging cycle. Li_2Te nanocrystals are more likely to form during the

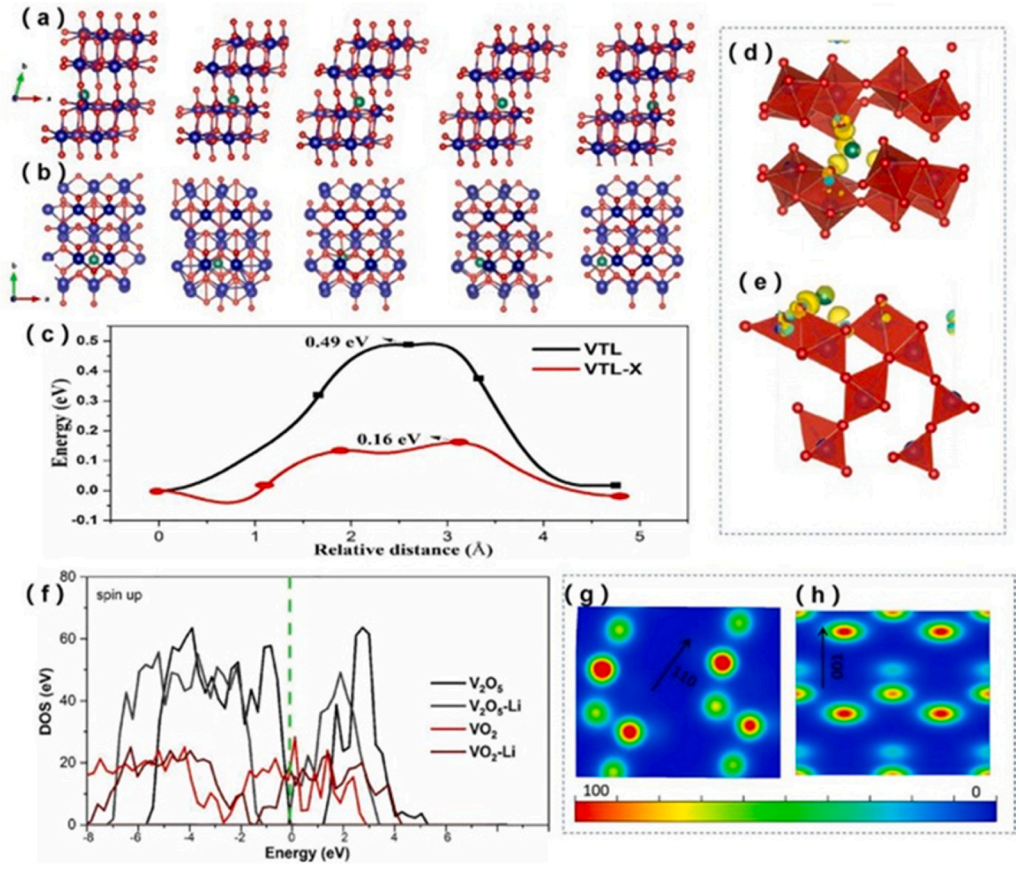

Fig. 5. DFT simulations of V_2O_5 and VO_2 for Li ion storage. Li^+ migration pathways along (a) V_2O_5 and (b) VO_2, (c) Corresponding energy barriers of Li^+ ions in V_2O_5 and VO_2. The corresponding deformation charge densities after one K atom inserting (d)V_2O_5 and (e)VO_2. Blue: charge depletion; yellow: charge accumulation. (f) The density of states for V_2O_5 and VO_2 before and after inserting one Li. The cross-sectional views of the electrostatic potential for (g) V_2O_5 and (h) VO_2. Reproduced with permission from Ref [113] Copyright 2022 Elsevier.

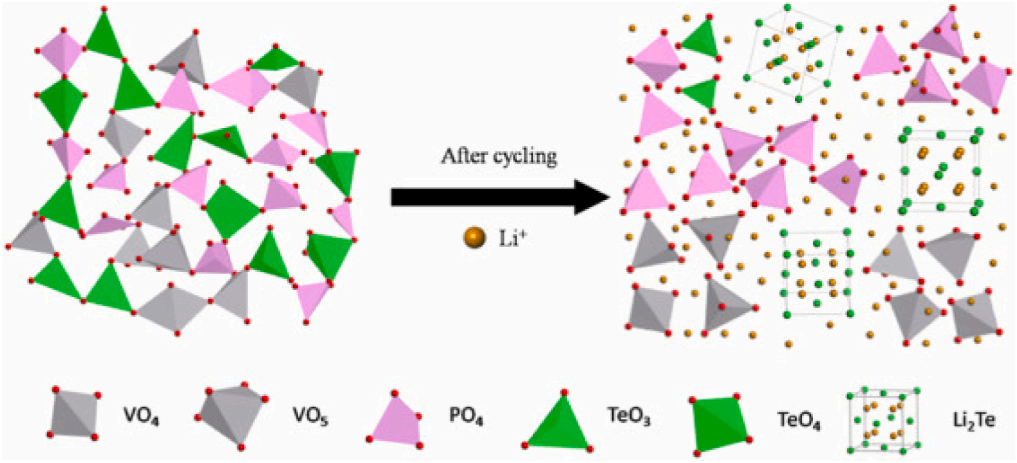

Fig. 6. Schematic representation of the local structural evolution induced by cycling. Reproduced with permission from Ref. [69] Copyright 2020, Elsevier.

discharge/charge cycle, particularly because of the reversible reaction between Te metal and the Li^+ ions added to the anode. The reversible capacity of the anode is greatly enhanced by the produced Li_2Te nanocrystals.

2.3. Other glass anodes

In addition to SnO_2 and V_2O_5, GeO_2, another kind of IV metal element germanium used for energy storage batteries, has also received extensive attention. Esper et al. [93] prepared flake glass-ceramic anode materials composed of SiO_2 and GeO_2, prepared precursor glass by melting quenching, and then made it into glass-ceramic by heat treatment. The 520 $mAhg^{-1}$ stable reversible capacity of SiO_2 and GeO_2 flake glass ceramic anode materials exhibits good capacity retention of 87% after 100 cycles. Wei-Qiang Han's team [71] demonstrated an amorphous hierarchical porous GeO_x nanostructure with a primary particle diameter of about 3.7 nm and a very stable capacity of about 1250 $mAhg^{-1}$ in 600 cycles. In addition, they also showed that the whole battery coupled with lithium $(NiCoMn)_{1/3}O_2$ cathode had high performance.

Iron phosphate glass as an anode material has also been widely studied. Qi et al. [73] studied the thermal and electrochemical properties of xFe_2O_3- (100-x) P_2O_5 glass (x = 20, 30, 40, and 50mol%) as anodes for lithium ion batteries. Glass was prepared by mechanical milling. 50FeP glass-ceramic anode annealed at 1033 K for 4 h provides a very high capacity (237$mAhg^{-1}$) times larger than pure 50FeP glass anode after 1000 cycles at 1Ag^{-1} The increase of 50FeP glass-ceramics capacity is closely related to the reduction of charge transfer resistance due to the formation of $Fe_3(P_2O_7)_2$ crystals containing both Fe^{2+} and Fe^{3+}. Iron phosphate glass ceramics have great potential as anode materials for advanced. Then the crystallization behavior of 50Fe-50P_2O_5glass in air and reduction atmosphere (5mol%H_2+95mol%Ar) and its effect on the performance of LiBs anode were studied [15]. The reduced glass-ceramic-based anode exhibits a capacity of 373 $mAhg^{-1}$ after 1000 cycles at the current density of 1Ag^{-1}, whereas the oxidized glass-ceramic based ones feature a capacity of 213 $mAhg^{-1}$ at the same current density. In addition, compared with untreated anode and anodized anode, the reduced glass-ceramic based anode has a higher rate of performance.

2.4. MOF amorphous anode

A new generation of lithium-ion batteries now uses metal-organic framework (MOF) as a high-energy anode material because of its thermochemical stability, high specific surface area, superior porosity, changeable pore size and shape, chemical function, and plenty of reaction sites [117]. However, during lithium insertion and deintercalation, the pore structure of crystalline MOFs would collapse, limiting their electrochemical efficiency. This issue can be somewhat resolved by MOF when it is in an amorphous condition. Most crystalline MOFs do not have a stable liquid state during heating. This is because most of them decompose before melting, accompanied by vaporization or carbonization of the ligand portion and oxidation of metal ions. This characteristic makes it impossible to prepare glass by melt quenching [25].

Mechanical milling or melting quenching can be used to create amorphous MOFs. Amorphous MOFs have different characteristics from crystalline MOFs. Additionally, the sol-gel approach can be used to directly generate amorphous MOFs. At present, only a few MOFs can be used to prepare glass by melting and quenching. As an alternative way of non-melting glassy MOFs, the transformation from crystal to glass can be directly induced by ball milling [117].

Several members of a subclass of MOFs, zeolite imidazole salt framework (ZIFs), have been proven to be melted and form liquid ZIF-62 $[M(Im)_{2-x}(bIm)_x]$ with the same composition as the crystalline parent material (Fig. 7), where $x \geq 0.05$, $M = Zn^{2+}$ or Co^{2+}, Im= $[C_3H_3N_2]^-$ and bIm= $[C_7H5N_2]^-$. ZIF liquid can be melted to form at about 430 °C. After quenching, this liquid will produce a glass (agZIF-62, ag=melt-quenched glass) with a continuous random network topology similar to amorphous SiO_2 [118].

Gao et al. [119] prepared CoZIF-62 (Co (Im) 1.75 (bIm) 0.25) glass by melting quenching and mechanical milling. The results showed that the melting and milling processes did not affect the chemical composition of Co-ZIF-62, but made its microstructure highly disordered. Then, the effect of the disorder of the ZIF structure on the electrochemical performance of the ZIF-based anode of lithium ion battery was studied. The quenched anode had a high lithium storage capacity (306$mAhg^{-1}$ after 1000 cycles at 2Ag^{-1}). Compared with the crystal cobalt Co-ZIF-62 and the high-energy ball-milled amorphous Co-ZIF-62, it had excellent cycle stability and excellent rate performance. The reason is that compared with other types of reticular glass (such as oxide glass), it is disordered at all length scales, such as short-range (0.5–0.8 nm), medium-ranee (0.8–2 nm), and long-range (>20 nm). Second, the coordination bond, which is significantly weaker than the covalent link and ionic bond in the inorganic glass, is used to build the connection between metal nodes and ligands. Thirdly, unlike ZIF crystal, the glass structure is likewise in a high metastable state and has greater potential energy. These three properties make ZIF glass more vulnerable to Li+ ion insertion and extraction at high current densities, boosting the capacity by increasing the number and size of Li^+ ion transfer channels as the cycle increases (Fig. 8). After 1000 cycles, the capacities of ZIF crystal, ZIF glass, and amorphous ZIF were 157, 188, and 306 $mAhg^{-1}$,

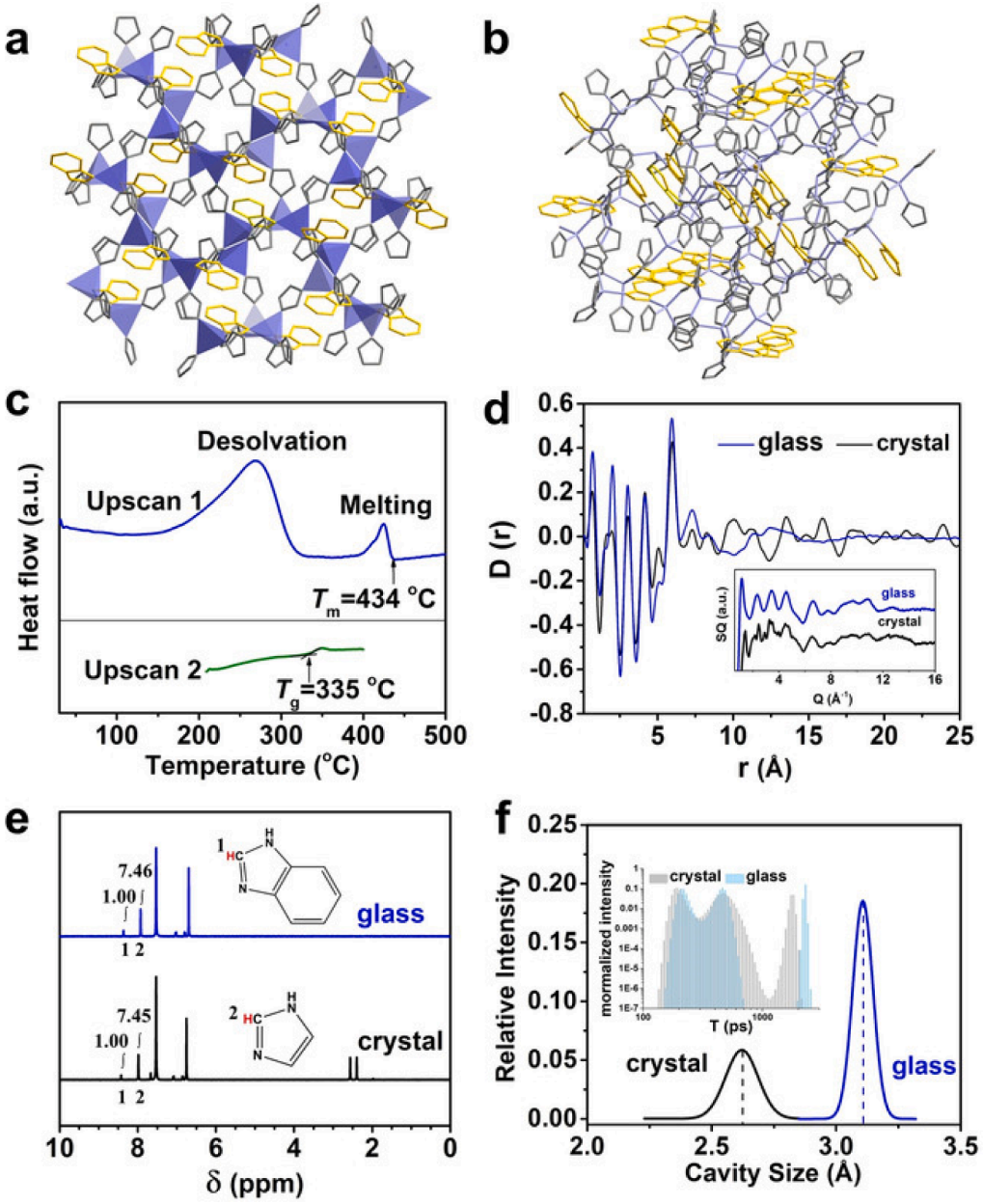

Fig. 7. (a) Characterization of ZIF-62 crystal structure. (b) ZIF-62 glass schematic. (c) DSC curve of ZIF-62. (d) The pair distribution function d (r) of ZIF-62 crystal and glass; the illustration shows the x-ray structural factor S (Q). (e) ^{1}H NMR spectra and pore size distribution of PALS in (f) ZIF-62crystal and glass. Reproduced with permission from Ref. [118] Copyright 2020, Wiley-VCH.

respectively.

During charge-discharge cycles, the majority of high-capacity crystal materials go through an irreversible phase transition and volume shift that causes unanticipated amorphization and loss of low-valent metal ions in the electrolyte. Additionally, the lithium diffusion is constrained by the crystal structure. Disordered materials may exhibit greater electrochemical performance than ordered polycrystalline materials, despite the fact that the majority of current research on electrode materials concentrates on crystal materials.

Another strategy, disordered/ordered engineering, was recently developed and demonstrated to be a strong method of improving the electrochemical performance of anode and cathode materials for lithium ion or sodium ion batteries. The disordered/ordered transitions were found in the glass anodes such as tin oxide, vanadium oxide, and iron oxide during charge and discharge, which affected the electrochemical performance. Despite these developments, the process of structural deterioration of negative MOF materials remains unknown, as does the influence of structural alterations on lithium storage performance. Understanding these effects will be extremely beneficial in the development of novel MOFs and other anode materials that can regulate and control structural changes to improve lithium storage and cycle stability. Gao et al. [76] used a simple and low-cost method to prepare porous aluminum-based MOF/graphene (AMG) composites and discussed the effect of structural changes of MOF during discharge/charge on the electrochemical performance of lithium ion batteries. After 100 cycles, most of the diffraction peaks of AMG disappeared, indicating that amorphous Al-MOF occurred in the discharge/charging cycle, that is, the ordered-disordered transition occurred, and finally long-range ordered disappeared (Fig. 9). AMG maintains impressive capacity of 484, 284, 267, and153mAhg^{-1} after 1000 cycles at 500, 800, 1000 and 2000 mAg^{-1},respectively. The AMG demonstrates a capacity improvement trend with continuous cycling up to 1000 cycles at current densities less

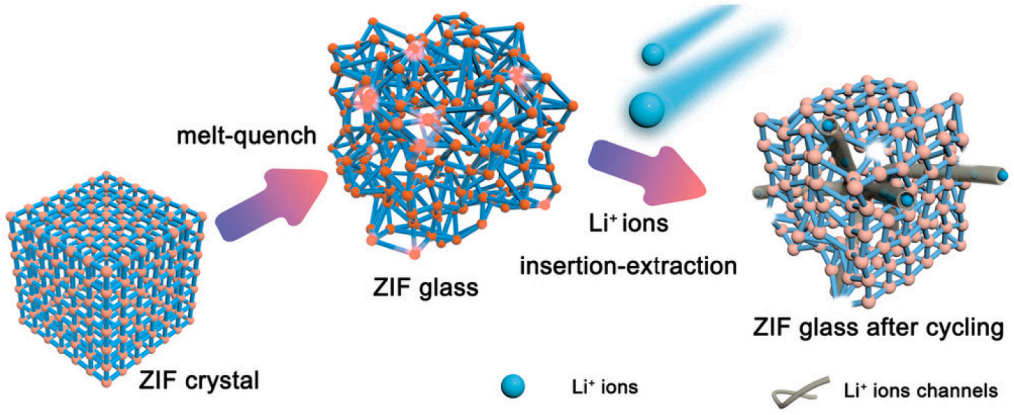

Fig. 8. The schematic representation of the structural origin of the capacity enhancement in the ZIF glass anode. Reproduced with permission from Ref [119] Copyright 2021, Wiley-VCH.

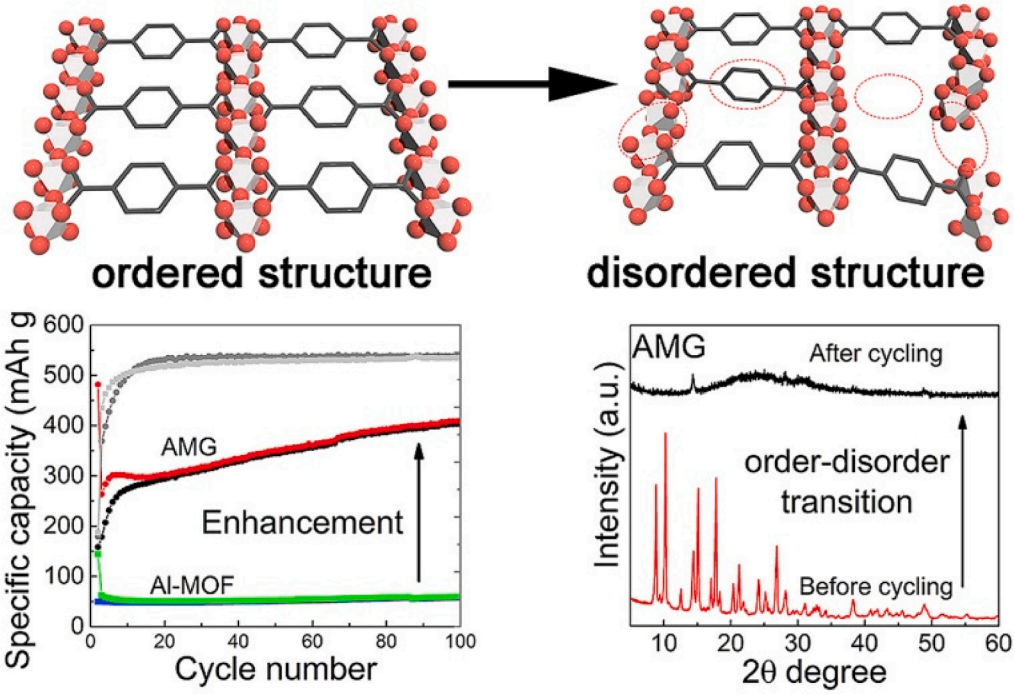

Fig. 9. AMG capacity and structure changes before and after charging. Reproduced with permission from Ref. [76] Copyright 2020, Elsevier.

than 1000 mAg^{-1}. This remarkable enhancement can be attributed to the disorder of lithium ion migration and storage channels in MOF crystals, and disorder is the main reason for lithium ion migration and storage channels. MOF particles maintain electronic conductivity through graphene sheets and current collectors. These sheets boost the electrical conductivity of the SEI layer and improve the migration kinetics and charge transfer reaction of Li^+ ions. The ordered and disorderly transition of MOF during lithium/etching is a useful way for improving the cyclic stability of MOF-containing anode materials, providing insight for future MOF anode material development.

In short, Due to the special network structure of glass, glassy anode materials have many unique advantages over crystalline materials. However, the capacity and cycle stability of the glassy anode need to be improved. Order-disorder engineering is a good strategy. The tin-based oxide glass, vanadium-based oxide glass and MOF glass introduced above all improve their capacity and cycle performance after forming nano-sized ordered structures. The disordered network structure can limit the volume change during the charge-discharge process, and the ordered nanocrystals can improve the capacity and cycle stability. The formation of ordered nano-grains inside the glass induced by heat treatment or charge-discharge is a way to improve the performance of the glass anode.

3. Glass cathode

Most cathode materials mainly undergo intercalation reaction. Lithium-ion transport efficiency is decreased in crystalline cathode materials due to the presence of grain boundaries. The majority of high-capacity crystalline materials experience irreversible volume and phase changes during charge/discharge cycles, which impair cycle performance or lower capacity. Although crystalline materials are the subject of the majority of studies on electrode materials, it is thought that disordered materials may perform more electrochemically than ordered polycrystalline materials.

Vanadium has multiple valence states, which makes vanadium-based materials can be used as both anode and cathode of the battery. Due of

vanadium's several oxidation states, vanadate glass, one of numerous glass cathode materials, has received much study. Transition metal vanadium oxides exhibit fascinating features in addition to electrochemical activity. For instance, the addition of V_2O_5 can enhance the conductivity of a binary glass system [120]. However, the vanadate glass becomes structurally unstable when charging and discharging because of the Jahn-Teller effect, which reduces capacity and shortens life. Different from vanadium oxide as anode material, the main reaction of vanadium oxide as cathode material is the reversible formation of lithium-oxygen-vanadium compounds with lithium ions. In recent years, numerous promising vanadate-glass cathode materials for lithium-ion batteries have been described (Table 2). These materials aim to increase the specific capacity and cycle stability of vanadate glass. Delaizir et al. [32] studied the glass component $25Li_2O$-$50V_2O_5$–$25P_2O_5$ as potential electrode materials. The glass composition's electrical and electrochemical characteristics were identified. The results show that the capacity is less than 80 $mAhg^{-1}$ at a 3–4.5 V potential window. The electronic conductivity of $2TeO_2$-V_2O_5 glass-ceramics with the crystallinity of 0–100 wt%, that is, from entirely amorphous to completely crystalline, was investigated by Kjeldsen [31]. Glass ceramics are made using heat treatment, whereas the glass is prepared using melting quenching method. The electronic conduction of $2TeO_2$-V_2O_5 glass ceramics is enhanced due to the shrinkage effect and percolation between particles. This shows that due to its electronic conductivity, $2TeO_2$-V_2O_5 glass ceramics is more appropriate as a cathode material for secondary batteries than $2TeO_2$-V_2O_5 glass. Li_2O-V_2O_5-B_2O_3 glass was first chosen as the positive glass by Afyon et al. [121]. Investigating the glass oxidation active system, utilizing the multivalent state of the transition metal vanadium, and stabilizing the vanadate group via the network to enhance the material's cycle stability. The initial capacity is as high as 327$mAhg^{-1}$ at a current density of 50 mAg^{-1} at 1.5–4.0 V.

A promising replacement for the cathode in high-capacity lithium-ion batteries is mixed polyanion (MP) glass. It is possible to create and investigate a variety of materials using phosphotes, borates, silicates, and other polyanion compositions as good glass formers [34].Vanadate glass cathode electrochemical performance can be increased by doping metal oxides. The "mixed network forming agent effect" will be created when an additional network forming agent is applied, and it will improve the electrochemical performance. The inclusion of Bi_2O_3 can alter the glass network structure in the vanadate glass system while simultaneously increasing conductivity. Li_2O-V_2O_5-B_2O_3-Bi_2O_3 quaternary glass cathode material was created by Chen et al. [122]. Using the melt quenching method, and the effect of the Bi_2O_3 content on the material's structure and stability over charge-discharge cycles was investigated. According to the findings, the capacity retention rate is approximately 90.0%, and the discharge capacity is approximately 300 $mAhg^{-1}$ after 10 cycles of charging and discharging at 50 mAg^{-1}. A high vanadium content Li_2O-V_2O_5-B_2O_3 glassy electrode material was created by Wang et al. [33]. To generate a disordered network structure, the Li_2O-V_2O_5-B_2O_3 glass was primarily connected with VO_4 and BO_3 structural units. The initial discharge capacity of the $20Li_2O$-$60V_2O_5$–$20B_2O_3$ glass cathode material was 168.6 mAg^{-1} at a current density of 100 mAg^{-1}. When 10% of the B_2O_3 was replaced with Fe_2O_3, the density and stability of the material increased. Furthermore, the addition of Fe_2O_3 increases the concentration of low valence V^{4+}, V^{3+}, and Fe^{2+} ions, which improves electrochemical performance. The cathode material composed of $20Li_2O$-$60V_2O_5$–$10B_2O_3$–$10Fe_2O_3$ had a much higher specific capacity. At a current density of 100 mAg^{-1}, the initial discharge capacity reached a maximum of 306.2 mAg^{-1} and fell to 120.3 mAg^{-1} after 100 cycles. Li_2O-V_2O_5-SiO_2-B_2O_3 quaternary glass was created by Zhao et al. [35]. using the melting-quenching technique. The structure and electrochemical characteristics of the glass material were investigated by varying the Si and B concentration. SiO_4, BO_3, and VO_6 serve as the primary structural constituents of the glass material, which together form a disordered glass network. Glass has the maximum V^{4+} concentration and the best electrochemical performance when Si and B content are 40% and 10%, respectively (LVSB10). The material was ball milled to further optimize the particle size in order to enhance cycle performance (LVSB10-b). The initial discharge capacity was 158.1 $mAhg^{-1}$ at a current density of 50 mAg^{-1} in the voltage range of 1.5–4.2 V, and the capacity retention rate after 100 cycles was 56.5%.

At present, there are few studies on amorphous cathode materials, but the cathode materials of glass and glass ceramics are very promising. The amorphous cathode can overcome the shortcomings of the crystalline cathode, such as irreversible phase transition and poor air stability. However, the amorphous cathode also has disadvantages such as poor cycleability. The formation of nanocrystals inside the glass and the addition of multiple anions to form a ' mixed anion effect ' is a feasible method to improve the glassy cathode.

4. Glass electrolyte

Due to its high level of safety and great energy density, all-solid-state lithium secondary batteries are regarded as the most potential next-generation energy storage device. The most important component of all solid lithium batteries is the solid electrolyte. Due to their strong conductivity, which is comparable to liquid electrolytes, sulfide solid electrolytes have received a lot of attention in the field of solid electrolytes. Some studied sulfide glass electrolytes are listed in Table 3. Due to its open network structure, the glassy solid electrolyte has a better

Table 3
Some glass electrolyte synthesis methods and room temperature conductivity.

Electrolyte	Phase	Method	Room temp. conductivity [Scm^{-1}]	Refs.
$80Li_2S$-$20P_2S_5$	Glass-ceramic	Mechanical milling	7.2×10^{-4}	[140]
$78Li_2S$-$22P_2S_5$	Glass-ceramic	Mechanical milling	1.78×10^{-3}	[141]
$70Li_2S$-$30P_2S_5$	Glass-ceramic	Melting quench	3.2×10^{-3}	[142]
$50Li_2SO_4$–$50Li_2CO_3$	Glass	Mechanical milling	6.3×10^{-7}	[143]
$2Li_2O$-SeO_2-B_2O_3	Glass	Melting quench	8×10^{-7}	[144]
$95(0.6L_2S$-$0.4SiS_2)$–$5Li_4SiO_4$	Glass	Melting quench	2×10^{-3}	[145]
$77(0.75Li_2S$-$0.25P_2S_5)_{33}LiBH_4$	Glass-ceramic	Mechanical milling	1.6×10^{-3}	[137]
$0.6(0.6Li_2S$-$0.4SiS_2)$ $0.4LiI$	Glass	Melting quench	1.78×10^{-3}	[126]

Table 2
Some glass cathode synthesis methods and Capacity.

Cathode	Physical condition	Method of combining	Capacity	Refs.
$25Li_2O$-$50V_2O_5$–$25P_2O_5$	Glass	Melting quench	75 mAhg-1 3–4.5 V 15 cycles	[32]
$20Li_2O$-$30V_2O_5$–$40SiO_2$–$10B_2O_3$	Glass	Melt-quenching	50mAg^{-1} 158.1 mAh/g	[35]
$20Li_2O$-$60V_2O_5$–$20B_2O_3$	Glass	Melt-quenching	120.3 $mAhg^{-1}$100cycles	[33]
$20Li_2O$-$60V_2O_5$–$10B_2O_3$–$10Fe_2O_3$	Glass	Melt-quenching	168.6$mAhg^{-1}$100cycles	[33]
Li_2O-V_2O_5-B_2O_3-Bi_2O_3	Glass	Melt-quenching	300 $mAhg^{-1}$10cycles	[122]
Li_2O–B_2O_3–V_2O_5	Glass	Melt-quenching	50mAg^{-1}260 $mAhg^{-1}$45cycles	[121]

conductivity than crystalline materials. Following are three crucial steps in the creation of high lithium-ion conductivity solid electrolyte glass: (1) oxide glass is transformed into sulfide glass; (2) combining sulfide and oxide anions, the so-called " mixed anion effect " is used to improve the conductivity and chemical stability; (3) glass-ceramics are formed by heat treatment to improve the conductivity.

4.1. Sulfide glass electrolytes

Sulfide electrolytes (S-SEs) originated from Pradel's study of Li_2S-SiS_2 in 1986. Sulfide glass is one of the earliest materials studied as lithium ion conductors. Sulfide glass electrolytes including Li_2S-SiS_2-glass [123–125], Li_2S-GeS_2glass [126,127], Li_2S-P_2S_5glass [126–130], and $Li_7P_3S_{11}$ glass-ceramics have high conductivity and wide electrochemical window. Firstly, since there is no anisotropic crystal structure in the material, the ion conduction pathway is isotropic. Second, the material's absence of crystallinity and grain significantly reduced grain boundary resistance, resulting in the glass's ionic conductivity being one to two orders of magnitude greater than that of the crystal phase with the same composition. Vulcanized glass is less difficult to manufacture and incorporate into solid-state batteries than oxide glass. The variety of composition, control over thickness, and mass manufacturing possibilities of sulfide glass electrolytes are enticing elements of industrial production. Because sulfides have a lower melting point than oxides, high temperatures are not required during processing, and cold pressure is frequently adequate to generate acceptable glass sulfides for lithium-ion conductivity. Sulfide glass is frequently produced via melt quenching (cooling with water or liquid nitrogen). A twin roller device is generally used to swiftly cool molten glass. As the concentration of lithium ions in the glass increases, the electrical conductivity of the glass may increase. Fig. 10 shows the dependence of the lithium concentration of some sulfides and oxides on the electrical conductivity at room temperature. Sulfide glass prepared by the melt quenching method can form thin film glass containing high concentrations of lithium. Mechanical milling of precursor materials can also produce high conductive glass. Compared with the melting quenching method, the mechanical milling method requires much less heat and can reduce the cost of large-scale production.

Because silicon is inexpensive and simple to make, including it in the solid electrolyte of all solid lithium ion batteries can reduce system costs. Because they exhibit the maximum ionic conductivity in lithium ion conductive glass, xLi_2S-$(100-x)SiS_2$ is the focus of research on glass as a solid electrolyte. In their study, Mori et al. [132] used RMC modeling and BVS imaging to visualize the three-dimensional atomic configuration and conduction path of lithium ions in xLi_2S-$(100-x)SiS_2$ glass (Fig. 11). The results show that some SiS_4 tetrahedral elements are connected by edge sharing (Si=*S*=Si bridge) and angle sharing (Si-S-Si

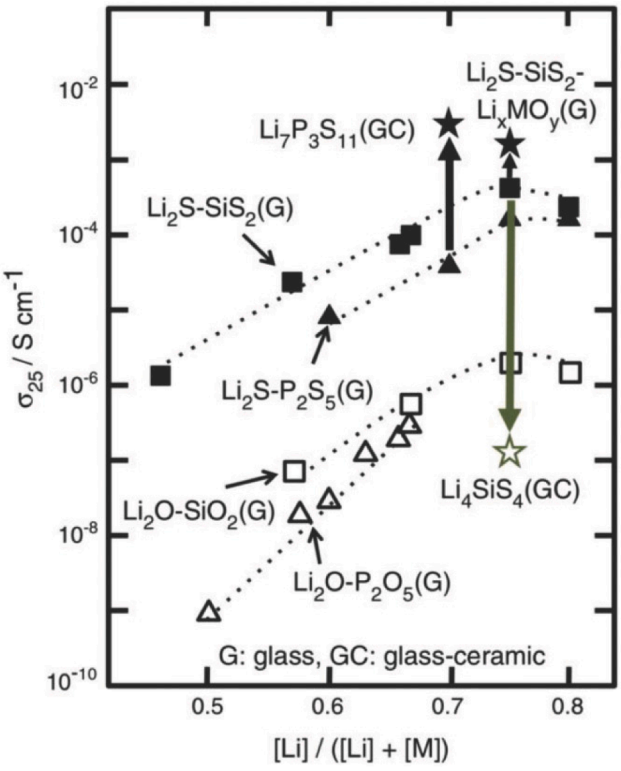

Fig. 10. Dependence of room-temperature ionic conductivity on lithium concentration for sulfide glass and glass-ceramic solid electrolytes. Reproduced with permission from Ref. [131]. Copyright 2012, Elsevier.

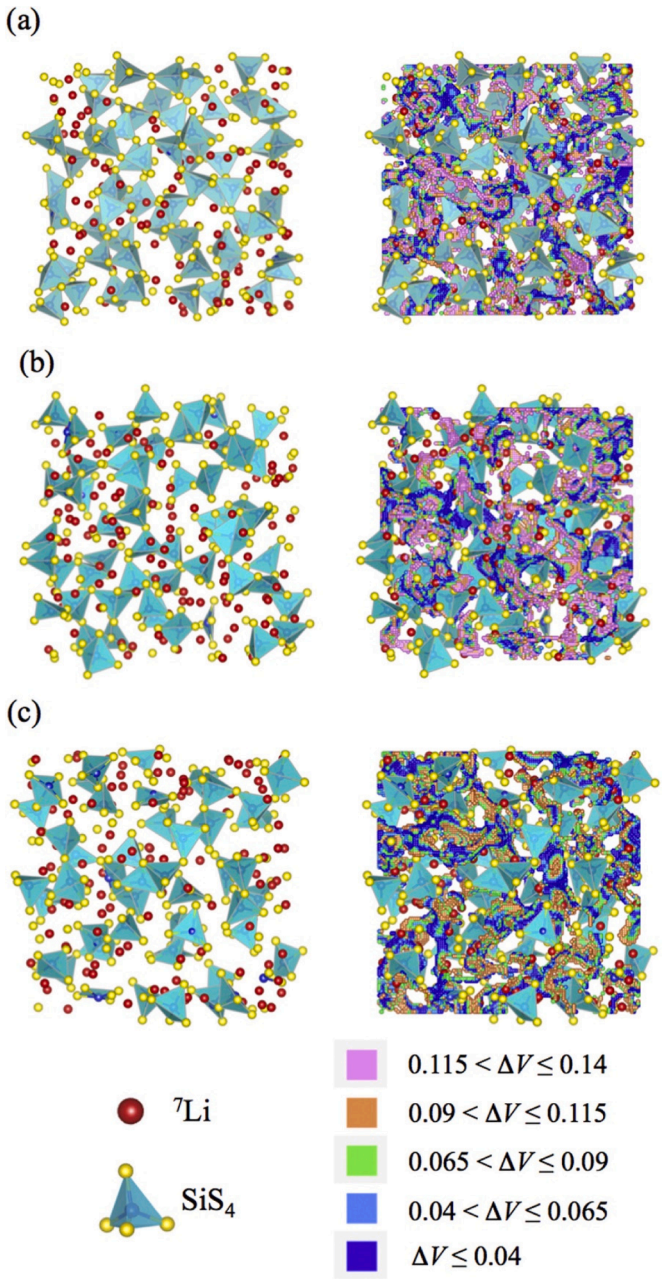

Fig. 11. Three-dimensional atomic configurations and conduction pathways of Li ions for (a) $(^7Li_2S)_{40}(SiS_2)_{60}$ glass, (b) $(^7Li_2S)_{50}(SiS_2)_{50}$ glass, and (c) $(^7Li_2S)_{60}(SiS_2)_{40}$ glass. Reproduced with permission from Ref. [132] Copyright 2020, Elsevier.

bridge). In addition, the polyhedron analysis of the ^{7}LiSn unit ($1 \leq n \leq 7$) found that each lithium ion was mainly surrounded by three or four S atoms in $r = 3.0$ Å (i. e., $N_{Li\text{-}S} = 3or4$).

It was found that the electrical conductivity was improved to a certain extent by heat treatment to crystallize the sulfide glass electrolyte into glass ceramics. To define the link between Li_2S-P_2S_5 glass electrolyte's ionic conductivity and crystallization behavior, Tsukasaki et al. [133] studied the crystallization process of $75Li_2S$-$25P_2S_5$ glass during heating and the precipitation of β-Li_3PS_4 nanocrystals, which did not grow with the increase of temperature. Due to the crystallization of $75Li_2S$-$25P_2S_5$ glass, the ionic conductivity increased at the beginning but decreased sharply above 180 °C.

Sulfide solid electrolytes, on the other hand, must be handled in an inert gas environment. One disadvantage of sulfide solid electrolytes is their low chemical stability in air. Water hydrolyzes them, releasing H_2S gas as a result. Effective inhibition of the production of H_2S gas in the atmosphere can be achieved by substituting an oxygen atom for a sulfur atom in a sulfide solid electrolyte. In particular, $xLi_2O\cdot(75-x)\ Li_2S$-$25P_2S_5$ (mol%) glass almost does not produce H_2S gas in the air. Tsukasaki et al. [134] added Li_2O to $75Li_2S$-$25P_2S_5$ glass to improve its chemical stability to water in the air. It was investigated how adding Li_2O affected the electrical and thermal characteristics of the $75Li_2S$-$25P_2S_5$ glass. With increasing Li_2O concentration, the crystallization temperature of $75Li_2S$-$25P_2S_5$ glass changes to the high temperature side, and the glass phase is stable throughout a wide temperature range. The thermal stability of the glass may be increased by swapping Li_2S for Li_2O, while the addition of Li_2O has no effect on the glass's electrical conductivity. The electrical conductivity exceeds 10^{-4} Scm^{-1}. The chemical stability of Li_2S-P_2S_5-P_2O_5 oxysulfide glass electrolytes was examined by Akitoshi Hayashi's team [135]. The effects of P_2O_5 replacing part of P_2S_5 on the chemical stability and ionic conductivity of glass structure modification were studied. In addition, the inhibitory effect of ZnO addition on the formation of H_2S in the prepared electrolyte was studied [136]. By mechanically ball milling, $75Li_2S$-(25-x) P_2S_5-xP_2O_5 glass electrolyte was created. The findings demonstrated that as P_2O_5 level rose, the ionic conductivity of oxygen sulfide glass electrolytes dropped. The rate of H_2S generation in the air-exposed glass is decreased when P_2O_5 is partially substituted for P_2S_5. In addition, adding 10 mol% ZnO in $x = 10$ glass can reduce the release of H_2S into the air. Adding metal oxides to Li_2S-P_2S_5 by ball milling can also improve its stability in air. The added metal oxides were used as the absorbent of H_2S through the following reactions:

$$M_xO_y + H_2S \rightarrow M_xS_y + H_2O \quad (4)$$

where M was Fe, Zn and Bi. Additionally, it has been claimed that Li_2O/LiI or P_2O_5 partially replacing Li_2S or P_2S_5 in Li_2S-P_2S_5 can also increase its stability.

4.2. Mixed anion effect improves the conductivity of the solid electrolyte

Due to the "mixed anion effect," mixing two distinct anions, such as sulfides and oxides, can be a useful technique to increase the conductivity of glass electrolytes. Yamauchi et al. [137] prepared (100-x) $(0.75Li_2S$-$0.25P_2S_5)$-$xLiBH_4$ glass electrolytes by mechanical milling. $LiBH_4$ was added to the sulfide glass matrix. The glass has a higher conductivity than $75Li_2S$-$25P_2S_5$ master glass, and its conductivity rises as the amount of $LiBH_4$ in the glass increases. The glass with $x = 33$ shows the highest conductivity of $1.6 \times 10^{-3}Scm^{-1}$ and a wide electrochemical window of up to 5 V. Adding lithium halide in glass electrolyte can improve the conductivity of glass. Ujiie et al. [138] studied the effect of LiI addition on the conductivity and precipitated crystals of Li_2S-P_2S_5 glass ceramics. (100-x) $(0.7Li_2S$-$0.3P_2S_5)\cdot$xLiI glass was prepared by mechanical milling method. To create glass ceramics, the synthesized lithium-containing glass was crystallized. By using cyclic voltammetry, the electrochemical stability of $70Li_2S$-$30P_2S_5$ glass containing LiI was investigated. According to the findings, $Li_7P_3S_{11}$ crystals formed in all glass-ceramics, but LiI did not combine with the crystal to create a solid solution. The conductivity of the glass rises as the LiI level does. When $x = 20$, the conductivity increases to $5.6 \times 10^{-4}Scm^{-1}$. $80(0.7Li_2S$-$0.3P_2S_5)\cdot20$LiI glass has a wide electrochemical window of up to 10 V compared with Li^+/Li. Kato et al. [139] studied the mechanical and electrical properties of Li_2S-P_2S_5-LiX ($X = I$, Br and Cl) glass electrolytes and assembled batteries using silicon electrodes. The results show that after LiI was added into 75Li2S-25P2S5 glass, the Young's modulus gradually decreased from 23 GPa to 19Gpa. In addition, fewer pores and grain boundaries were observed in the powder-pressed pellets of $Li_2S-P_2S_5$ glasses with lithium halides. All-solid-state batteries using Si electrodes and glass electrolytes with lithium halides exhibited a larger capacity of 20 cycles compared to those without lithium halides. These results provide guidelines for the construction of all-solid-state batteries from the viewpoint of the mechanical properties of solid electrolytes (Fig. 12).

In general, sulfide glass is a very useful direction for the development of solid electrolytes. Sulfide glass can also improve the conductivity by adding a variety of anions and using the ' mixed anion effect '.

5. Conclusions and prospects

The next generation battery system requires increased capacity, improved safety, and improved cycle performance, which necessitates the development of new electrode and electrolyte materials. Glass's grain boundary free properties, open network structure, and tunable composition have garnered a lot of attention. Currently being investigated materials for glass anodes and glass electrolytes can offer high power, good safety, and cycle durability. Glass can be made by melting quenching or mechanical milling, and glass ceramics can be made by heat treatment under appropriate conditions, which can improve glass conductivity.

Tin oxide glass, vanadium oxide glass, iron phosphate glass, germanium-based glass, and amorphous MOF materials can provide higher capacity and stability than carbon anodes. These glasses' disordered/ordered transitions during charge/discharge have also piqued the interest of researchers. The use of disordered/ordered transitions in a reasonable manner can improve the capacity and cycling performance of glass anodes. Vanadate glass has been extensively researched as a cathode material. Doping metal oxides improve the electrochemical performance of a vanadate glass cathode. Using the 'mixed network forming agent effect,' appropriately incorporating phosphate, borate, silicate, and other polyanion combinations as network forming agents can increase electrochemical performance. Sulfide solid electrolytes are potential materials for increasing the performance of solid-state batteries. Solid state batteries provide increased energy density and enhanced safety by replacing traditional liquid electrolytes with lithium metal anodes. The chemical compositions of sulfide glass and microcrystal glass are essentially infinite, and their characteristics may be customized by carefully mixing glass forming agents and modifiers. The addition of oxides can reduce the production of H_2S, improving battery stability. The addition of halides can improve electrolyte conductivity. Glass's "mixed anion effect" can significantly improve the conductivity and safety performance of sulfide glass electrolytes.

In conclusion, the production of innovative glass and microcrystalline glass is a new trend in the development of cathode, anode, and solid electrolyte materials for the following generation of high-capacity batteries. The currently being developed amorphous materials could offer great power density, good safety, and cycle durability. Consequently, as the upcoming battery technology, they might be a promising replacement for lithium-ion batteries. Future SIB technology can be improved as a green battery technology with a little work in this area. As a result, it can lower operational expenses and address technical issues. Successful initiatives will guarantee that the rest of the world and fast-growing nations experience major economic and environmental benefits.

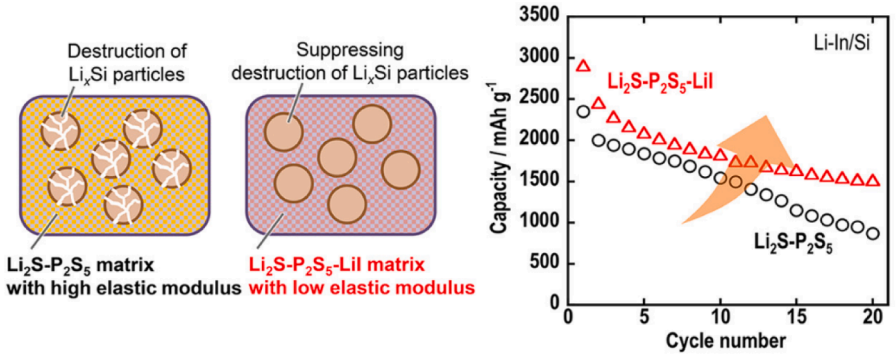

Fig. 12. Lithium iodide reduces the elastic modulus of glass electrolyte and increases the battery capacity. Reproduced with permission from Ref. [139] Copyright 2018, Elsevier.

Declaration of Competing Interest

The authors declare that they have no known competing financial interests or personal relationships that could have appeared to influence the work reported in this paper.

Data availability

The authors are unable or have chosen not to specify which data has been used.

Acknowledgments

This work was financially supported by the National Natural Science Foundation of China (NSFC) (52274295), Natural Science Foundation of Hebei Province (E2020501001, E2021501029, A2021501007, E2022501028, E2022501029), The Natural Science Foundation-Steel, the Iron Foundation of Hebei Province (No. E2022501030), S&T Program of Hebei (22567627H), the Science and Technology Project of Hebei Education Department (ZD2022158), the Central Guided Local Science and Technology Development Fund Project of Hebei province (226Z4401G), 2023 Hebei Provincial Postgraduate Student Innovation Ability training funding project (CXZZBS2023163, CXZZSS2023195).

References

[1] Y.K. Sun, Publishing electrochemical energy storage papers, ACS Energy Lett. 1 (2016) 771–772.
[2] J.B. Goodenough, Y. Kim, Challenges for rechargeable Li batteries, Chem. Mater. 22 (2010) 587–603.
[3] S. Choi, G. Wang, Advanced lithium-ion batteries for practical applications: technology, development, and future perspectives, Adv. Mater. Technol. 3 (2018).
[4] J. Xu, X. Cai, S. Cai, Y. Shao, C. Hu, S. Lu, S. Ding, High-energy lithium-ion batteries: recent progress and a promising future in applications, Energy Environ. Mater. (2022) e12450.
[5] Z.H. Fu, X. Chen, Q. Zhang, Review on the lithium transport mechanism in solid-state battery materials, Wiley Interdiscipl. Rev. Comput. Molecular Sci. (2023) 13.
[6] J. Lopez, J. Villarreal, J. Cantu, J. Parsons, M. Alcoutlabi, Metal sulfide/carbon composite fibers as anode materials for lithium ion batteries, SELECTED PROCEEDINGS FROM THE 233RD ECS MEETING, in: , 2018, pp. 275–284.
[7] V. Oleshko, S. Takeuchi, E. Bittle, Investigation of solid-state chemical lithiation of single crystalline silicon thin window anodes by analytical scanning and transmission electron microscopy, Microsc. Microanal. 26 (2020) 1448–1450.
[8] S. Jiao, J. Zheng, Q. Li, X. Li, M.H. Engelhard, R. Cao, J.G. Zhang, W. Xu, Behavior of lithium metal anodes under various capacity utilization and high current density in lithium metal batteries, Joule 2 (2018) 110–124.
[9] S. Gandi, W. Mekprasart, W. Pecharapa, D.P. Dutta, C. Jayasankar, B.R. Ravuri, Na–Ge glass anode network mixed with bismuth oxide nanocrystallites: a high capacity anode material for use in advanced sodium-ion battery design, Mater. Chem. Phys 242 (2020), 122568.
[10] J.R. Rodriguez, Z. Qi, H. Wang, M.Y. Shalaginov, C. Goncalves, M. Kang, K. A. Richardson, J. Guerrero-Sanchez, M.G. Moreno-Armenta, V.G. Pol, $Ge_2Sb_2Se_5$ glass as high-capacity promising lithium-ion battery anode, Nano Energy 68 (2020), 104326.
[11] S. Basu, N. Koratkar, Y. Shi, Structural transformation and embrittlement during lithiation and delithiation cycles in an amorphous silicon electrode, Acta Mater. 175 (2019) 11–20.
[12] M. Ma, J. Zhang, W. Shen, S. Guo, Cladding transition metal oxide particles with graphene oxide sheets: an efficient protocol to improve their structural stability and lithium ion diffusion rate, J. Solid State Electrochem. 23 (2019) 2969–2977.
[13] P. Lu, F. Ding, Z. Xu, J. Liu, X. Liu, Q. Xu, Study on (100-x)(70Li_2S-30P_2S_5)-xLi_2ZrO_3 glass-ceramic electrolyte for all-solid-state lithium-ion batteries, J. Power Sources 356 (2017) 163–171.
[14] T. Nagakane, H. Yamauchi, K. Yuki, M. Ohji, A. Sakamoto, T. Komatsu, T. Honma, M. Zou, G. Park, T. Sakai, Glass-ceramic $LiFePO_4$ for lithium-ion rechargeable battery, Solid State Ionics 206 (2012) 78–83.
[15] S. Qi, X. Li, Y. Yue, Y. Zhang, Iron-phosphate glass-ceramic anodes for lithium-ion batteries, Int. J. Appl. Glass Sci. 13 (2022) 420–428.
[16] A. Raskovalov, E. Il'ina, N. Saetova, S. Pershina, The all-solid-state battery with vanadate glass-ceramic cathode, Ionics 24 (2018) 3299–3304 (Kiel).
[17] Z. Liang, C. Qu, W. Guo, R. Zou, Q. Xu, Pristine metal–organic frameworks and their composites for energy storage and conversion, Adv. Mater. 30 (2018), 1702891.
[18] X. Zhang, P. Dong, M.K. Song, Metal– organic frameworks for high-energy lithium batteries with enhanced safety: recent progress and future perspectives, Batt. Supercaps 2 (2019) 591–626.
[19] B. Cui, G. Fu, Process of metal–organic framework (MOF)/covalent–organic framework (COF) hybrids-based derivatives and their applications on energy transfer and storage, Nanoscale 14 (2022) 1679–1699.
[20] G. Fang, J. Zhou, Y. Cai, S. Liu, X. Tan, A. Pan, S. Liang, Metal–organic framework-templated two-dimensional hybrid bimetallic metal oxides with enhanced lithium/sodium storage capability, J. Mater. Chem. A 5 (2017) 13983–13993.
[21] Y. Zhao, J. Liu, M. Horn, N. Motta, M. Hu, Y. Li, Recent advancements in metal organic framework based electrodes for supercapacitors, Sci. China Mater. 61 (2018) 159–184.
[22] C. Gao, P. Wang, Z. Wang, S.K. Kær, Y. Zhang, Y. Yue, The disordering-enhanced performances of the Al-MOF/graphene composite anodes for lithium ion batteries, Nano Energy 65 (2019), 104032.
[23] C. Gao, Z. Jiang, S. Qi, P. Wang, L.R. Jensen, M. Johansen, C.K. Christensen, Y. Zhang, D.B. Ravnsbæk, Y. Yue, Metal-organic framework glass anode with an exceptional cycling-induced capacity enhancement for lithium-ion batteries, Adv. Mater. 34 (2022), 2110048.
[24] A.M. Bumstead, I. Pakamorė, K.D. Richards, M.F. Thorne, S.S. Boyadjieva, C. Castillo-Blas, L.N. McHugh, A.F. Sapnik, D.S. Keeble, D.A. Keen, Post-synthetic modification of a metal–organic framework glass, Chem. Mater. 34 (2022) 2187–2196.
[25] J. Fonseca, T. Gong, L. Jiao, H.L. Jiang, Metal–organic frameworks (MOFs) beyond crystallinity: amorphous MOFs, MOF liquids and MOF glasses, J. Mater. Chem. A 9 (2021) 10562–10611.
[26] L. Longley, C. Calahoo, R. Limbach, Y. Xia, J.M. Tuffnell, A.F. Sapnik, M. F. Thorne, D.S. Keeble, D.A. Keen, L. Wondraczek, Metal-organic framework and inorganic glass composites, Nat. Commun. 11 (2020) 5800.
[27] N. Nitta, F. Wu, J.T. Lee, G. Yushin, Li-ion battery materials: present and future, Materials Today 18 (2015) 252–264.
[28] J. Li, S. Zhao, X. Wu, L. Yu, E. Zhao, C. Nan, Structure and electrochemical properties of C-coated Li_2O–V_2O_5–P_2O_5 glass-ceramic as cathode material for lithium-ion batteries, Funct. Mater. Lett. (2019).
[29] T.K. Pietrzak, J.E. Garbarczyk, I. Gorzkowska, M. Wasiucionek, J.L. Nowinski, S. Gierlotka, R. Jozwiak, Correlation between electrical properties and microstructure of nanocrystallized V_2O5-P_2O_5 glasses, J. Power Sources 194 (2009) 73–80.
[30] H. Park, W. Lee, R. Thangavel, W. Oh, B.S. Jin, W.S. Yoon, Enhancing electrochemical performance by triggering a local structure distortion in lithium vanadium phosphate cathode for Li ion batteries, J. Mater. Chem. A 10 (2022) 25129–25139.

[31] J. Kjeldsen, Y. Yue, C.B. Bragatto, A.C.M. Rodrigues, Electronic conductivity of vanadium-tellurite glass-ceramics, J. Non Cryst. Solids 378 (2013) 196–200.
[32] G. Delaizir, V. Seznec, P. Rozier, C. Surcin, P. Salles, M. Dolle, Electrochemical performances of vitreous materials in the system Li_2O-V_2O_5-P_2O_5 as electrode for lithium batteries, Solid State Ionics 237 (2013) 22–27.
[33] H. Wang, J. Li, Y. Yin, J. Chen, L. Wang, P. Zhang, X. Lai, B. Yue, X. Hu, D. He, Effects of V_2O_5 and Fe_2O_3 on the structures and electrochemical performances of Li_2O-V_2O_5-B_2O_3 glass materials in lithium-ion batteries, J. Alloys Compd. 879 (2021).
[34] A.K. Kercher, J.O. Ramey, K.J. Carroll, J.O. Kiggans, N.J. Dudney, R.A. Meisner, L.A. Boatner, G.M. Veith, Mixed polyanion glass cathodes: iron phosphate vanadate glasses, J. Electrochem. Soc. 161 (2014) A2210–A2215.
[35] E.L. Zhao, S.X. Zhao, X. Wu, J.W. Li, L.Q. Yu, C.W. Nan, G. Cao, Electrochemical performance of Li_2O-V_2O_5-SiO_2-B_2O_3 glass as cathode material for lithium ion batteries, J. Mater. 5 (2019) 663–669.
[36] J.B. Goodenough, Rechargeable batteries: challenges old and new, J. Solid State Electrochem. 16 (2012) 2019–2029.
[37] H. Jia, W. Xu, Nonflammable nonaqueous electrolytes for lithium batteries, Curr. Opin. Electrochem. 30 (2021), 100781.
[38] L. Han, C.T. Hsieh, B.C. Mallick, J. Li, Y.A. Gandomi, Recent progress and future prospects of atomic layer deposition to prepare/modify solid-state electrolytes and interfaces between electrodes for next-generation lithium batteries, Nanoscale Adv. 3 (2021) 2728–2740.
[39] L. Xu, J. Li, H. Shuai, Z. Luo, B. Wang, S. Fang, G. Zou, H. Hou, H. Peng, X. Ji, Recent advances of composite electrolytes for solid-state Li batteries, J. Energy Chem. 67 (2022) 524–548.
[40] X. Wang, R. Kerr, F. Chen, N. Goujon, J.M. Pringle, D. Mecerreyes, M. Forsyth, P. C. Howlett, Toward high-energy-density lithium metal batteries: opportunities and challenges for solid organic electrolytes, Adv. Mater. 32 (2020), 1905219.
[41] Y.S. Choi, J.C. Lee, Electronic and mechanistic origins of the superionic conductivity of sulfide-based solid electrolytes, J. Power Sources 415 (2019) 189–196.
[42] Y. Fujii, A. Miura, N.C. Rosero-Navarro, M. Higuchi, K. Tadanaga, FePS3 electrodes in all-solid-state lithium secondary batteries using sulfide-based solid electrolytes, Electrochim. Acta 241 (2017) 370–374.
[43] D. Liu, W. Zhu, Z. Feng, A. Guerfi, A. Vijh, K. Zaghib, Recent progress in sulfide-based solid electrolytes for Li-ion batteries, Mater. Sci. Eng. B 213 (2016) 169–176.
[44] Q. Zhang, D. Cao, Y. Ma, A. Natan, P. Aurora, H. Zhu, Sulfide-based solid-state electrolytes: synthesis, stability, and potential for all-solid-state batteries, Adv. Mater. 31 (2019), 1901131.
[45] A. Hayashi, N. Masuzawa, S. Yubuchi, F. Tsuji, C. Hotehama, A. Sakuda, M. Tatsumisago, A sodium-ion sulfide solid electrolyte with unprecedented conductivity at room temperature, Nat. Commun. 10 (2019) 5266.
[46] X. Sun, Y. Sun, F. Cao, X. Li, S. Sun, T. Liu, J. Wu, Preparation, characterization and ionic conductivity studies of composite sulfide solid electrolyte, J. Alloys Compd 727 (2017) 1136–1141.
[47] M.K. Tufail, L. Zhou, N. Ahmad, R. Chen, M. Faheem, L. Yang, W. Yang, A novel air-stable $Li_7Sb_{0.05}P_{2.95}S_{10.5}I_{0.5}$ superionic conductor glass-ceramics electrolyte for all-solid-state lithium-sulfur batteries, Chem. Eng. J 407 (2021), 127149.
[48] A. Hayashi, H. Muramatsu, T. Ohtomo, S. Hama, M. Tatsumisago, Improvement of chemical stability of Li_3PS_4 glass electrolytes by adding M_xO_y (M= Fe, Zn, and Bi) nanoparticles, J. Mater. Chem. A 1 (2013) 6320–6326.
[49] G. Liu, D. Xie, X. Wang, X. Yao, S. Chen, R. Xiao, H. Li, X. Xu, High air-stability and superior lithium ion conduction of $Li_{3+3x}P_{1-x}Zn_xS_{4-x}O_x$ by aliovalent substitution of ZnO for all-solid-state lithium batteries, Energy Storage Mater. 17 (2019) 266–274.
[50] T. Ohtomo, A. Hayashi, M. Tatsumisago, K. Kawamoto, Characteristics of the Li_2O–Li_2S–P_2S_5 glasses synthesized by the two-step mechanical milling, J. Non-Cryst. Solids 364 (2013) 57–61.
[51] A. Hayashi, T. Konishi, K. Tadanaga, T. Minami, M. Tatsumisago, Preparation and characterization of SnO–P_2O_5 glasses as anode materials for lithium secondary batteries, J. Non-Cryst. Solids 345 (2004) 478–483.
[52] H. Kondo, T. Honma, T. Komatsu, Synthesis and morphology of metal Sn particles in SnO–P_2O_5 glasses and their battery anode performance, J. Non-Cryst. Solids 402 (2014) 153–159.
[53] T. Konishi, A. Hayashi, K. Tadanaga, T. Minami, M. Tatsumisago, Electrochemical performance and structural change during charge–discharge reaction of SnO–P_2O_5 glassy electrodes in rechargeable lithium batteries, J. Non-Cryst. Solids 354 (2008) 380–385.
[54] A. Saitoh, R.K. Brow, U. Hoppe, G. Tricot, S. Anan, H. Takebe, The structure and properties of xZnO–(67-x) SnO–P_2O_5 glasses:(I) optical and thermal properties, Raman and infrared spectroscopies, J. Non-Cryst. Solids 484 (2018) 132–138.
[55] Y. Xia, M.A. Marple, I. Hung, Z. Gan, S. Sen, Network Structure and Connectivity in SnO–P_2O_5 Glasses: results from 2D ^{31}P and ^{119}Sn NMR Spectroscopy, J. Phys. Chem. B 122 (2018) 7416–7425.
[56] A. Hayashi, M. Nakai, H. Morimoto, T. Minami, M. Tatsumisago, Mechanochemical synthesis of SnO-B_2O_3 glassy anode materials for rechargeable lithium batteries, J. Mater. Sci. 39 (2004) 5361–5364.
[57] A. Hayashi, M. Nakai, M. Tatsumisago, T. Minami, Y. Himei, Y. Miura, M. Katada, Structural investigation of SnO–B_2O_3 glasses by solid-state NMR and X-ray photoelectron spectroscopy, J. Non-Cryst. Solids 306 (2002) 227–237.
[58] M. Nakai, A. Hayashi, H. Morimoto, M. Tatsumisago, T. Minami, Preparation and characterization of SnO-based glasses as anode materials for lithium secondary batteries, J. Ceram. Soc. Jpn. 109 (2001) 1010–1016.
[59] R. Barde, S. Waghuley, dc Electrical conductivity of V_2O_5-P_2O_5 binary glassy systems, J. Phys. Conf. Ser. (2012), 012019.
[60] M. Du, K. Huang, Y. Guo, Z. Xie, H. Jiang, C. Li, Y. Chen, High specific capacity lithium ion battery cathode material prepared by synthesizing vanadate–phosphate glass in reducing atmosphere, J. Power Sources 424 (2019) 91–99.
[61] H. Hirashima, K. Nishii, T. Yoshida, Electrical Conductivity of TiO_2-V_2O_5-P_2O_5 Glasses, J. Am. Ceram. Soc. 66 (1983) 704–708.
[62] A. Ivon, V. Kolbunov, I. Chernenko, Conductivity stabilization by metal and oxide additives in ceramics on the basis of VO_2 and glass V_2O_5–P_2O_5, J. Non-Cryst. Solids 351 (2005) 3649–3654.
[63] A. Raskovalov, S. Belyakov, N. Saetova, Proton transfer in V_2O_5–P_2O_5 glasses, J. Phys. Conf. Ser. (2021), 012013.
[64] S. Wu, D. Wang, Y. Zhong, X. Fang, Y. Chen, H. Jiang, C. Li, Y. Wang, Dynamic characterization of structural relaxation in V_2O_5–P_2O_5 bulk oxide glass, Phys. Chem. Chem. Phys. 21 (2019) 14879–14886.
[65] J. Fan, Y. Zhang, G. Li, Y. Yue, Tellurium nanoparticles enhanced electrochemical performances of TeO_2-V_2O_5-Al_2O_3 glass anode for Lithium-ion batteries, J. Non-Cryst. Solids 521 (2019), 119491.
[66] Y. Zhang, P. Wang, G. Li, J. Fan, C. Gao, Z. Wang, Y. Yue, Clarifying the charging induced nucleation in glass anode of Li-ion batteries and its enhanced performances, Nano Energy 57 (2019) 592–599.
[67] Y. Zhang, P. Wang, T. Zheng, D. Li, G. Li, Y. Yue, Enhancing Li-ion battery anode performances via disorder/order engineering, Nano Energy 49 (2018) 596–602.
[68] Z. Jiang, S. Qi, C. Gao, X. Li, Y. Zhang, Y. Yue, Water enables a performance jump of glass anode for lithium-ion batteries, J. Non-Cryst. Solids 576 (2022), 121225.
[69] Z. Jiang, T. Zhao, J. Ren, Y. Zhang, Y. Yue, NMR evidence for the charge-discharge induced structural evolution in a Li-ion battery glass anode and its impact on the electrochemical performances, Nano Energy 80 (2021), 105589.
[70] S. Liu, W. Tang, J. Ma, Y. Zhang, Y. Yue, Li_2TiSiO_5 glass ceramic as anode materials for high-performance lithium-ion batteries, ACS Appl. Energy Mater. 3 (2020) 9760–9768.
[71] S.H. Choi, S.J. Lee, H.J. Kim, S.B. Park, J.W. Choi, Li_2O–B_2O_3–GeO_2 glass as a high performance anode material for rechargeable lithium-ion batteries, J. Mater. Chem. A 6 (2018) 6860–6866.
[72] J.D. Esper, Y. Zhuo, M.K. Barr, T. Yokosawa, E. Spiecker, D. de Ligny, J. Bachmann, W. Peukert, S. Romeis, Shape-anisotropic cobalt-germanium-borate glass flakes as novel Li-ion battery anodes, Powder Technol. 363 (2020) 218–231.
[73] S. Qi, X. Li, Z. Jiang, J. Zhang, Z. Shan, Y. Zhang, Enhancing glass anode performance for lithium-ion batteries via crystallization, J. Am. Ceram. Soc. 105 (2022) 1001–1009.
[74] M. Stepniewska, M.B. Østergaard, C. Zhou, Y. Yue, Towards large-size bulk ZIF-62 glasses via optimizing the melting conditions, J. Non-Cryst. Solids 530 (2020), 119806.
[75] M.F. Thorne, A.F. Sapnik, L.N. McHugh, A.M. Bumstead, C. Castillo-Blas, D. S. Keeble, M.D. Lopez, P.A. Chater, D.A. Keen, T.D. Bennett, Glassy behaviour of mechanically amorphised ZIF-62 isomorphs, Chem. Commun. 57 (2021) 9272–9275.
[76] C. Gao, Z. Jiang, P. Wang, L.R. Jensen, Y. Zhang, Y. Yue, Optimized assembling of MOF/SnO_2/Graphene leads to superior anode for lithium ion batteries, Nano Energy 74 (2020), 104868.
[77] A. Fukushima, A. Hayashi, H. Yamamura, M. Tatsumisago, Mechanochemical synthesis of high lithium ion conducting solid electrolytes in a Li_2S-P_2S_5-Li_3N system, Solid State Ionics 304 (2017) 85–89.
[78] P. Mirmira, J. Zheng, P. Ma, C.V. Amanchukwu, Importance of multimodal characterization and influence of residual Li2S impurity in amorphous Li_3PS_4 inorganic electrolytes, J. Mater. Chem. A 9 (2021) 19637–19648.
[79] F. Mizuno, A. Hayashi, K. Tadanaga, T. Minami, M. Tatsumisago, All-solid-state lithium secondary batteries using Li_2S–SiS_2–Li_4SiO_4 glasses and Li_2S–P_2S_5 glass ceramics as solid electrolytes, Solid State Ionics 175 (2004) 699–702.
[80] H. Nagata, J. Akimoto, Excellent deformable oxide glass electrolytes and oxide-type all-solid-state Li_2S-Si batteries employing these electrolytes, ACS Appl. Mater. Interfaces 13 (2021) 35785–35794.
[81] J. Saienga, Y. Kim, B. Campbell, S.W. Martin, Preparation and characterization of glasses in the LiI+Li2S+GeS2+Ga2S3 system, Solid State Ionics 176 (2005) 1229–1236.
[82] H. Tsukasaki, H. Morimoto, S. Mori, Ionic conductivity and thermal stability of Li_2O-Li_2S-P_2S_5 oxysulfide glass, Solid State Ionics (2020) 347.
[83] Y. Zhang, R. Chen, T. Liu, Y. Shen, Y. Lin, C.W. Nan, High capacity, superior cyclic performances in all-solid-state lithium-ion batteries based on $78Li_{(2)}S$-$22P_{(2)}S_{(5)}$ Glass-ceramic electrolytes prepared via simple heat treatment, ACS Appl. Mater. Interfaces 9 (2017) 28542–28548.
[84] V. Chaudoy, J. Jacquemin, F. Tran-Van, M. Deschamps, F. Ghamouss, Effect of mixed anions on the transport properties and performance of an ionic liquid-based electrolyte for lithium-ion batteries, Pure Appl. Chem. 91 (2019) 1361–1381.
[85] H.H. Heenen, J. Voss, C. Scheurer, K. Reuter, A.C. Luntz, Multi-ion conduction in Li_3OCl glass electrolytes, J. Phys. Chem. Lett. 10 (2019) 2264–2269.
[86] Y. Chen, X. Chen, Y. Zhang, A comprehensive review on metal-oxide nanocomposites for high-performance lithium-ion battery anodes, Energy Fuels 35 (2021) 6420–6442.
[87] L.Q. Yu, S.X. Zhao, X. Wu, J.W. Li, E.L. Zhao, G.D. Wei, Lithium ion storage behaviors of (100-x) V_2O_5-(x) P_2O_5 glass as novel anode materials for lithium ion battery, J. Alloys Compd. 810 (2019).
[88] S. Liu, V. Boffa, D. Yang, Z. Fan, F. Meng, Y. Yue, Clarifying the gel-to-glass transformation in Al_2O_3-SiO_2 systems, J. Non-Cryst. Solids 492 (2018) 77–83.

[89] H. Morimoto, M. Nakai, M. Tatsumisago, T. Minami, Mechanochemical synthesis and anode properties of SnO-based amorphous materials, J. Electrochem. Soc 146 (1999) 3970–3973.
[90] H. Yamauchi, G. Park, T. Nagakane, T. Honma, T. Komatsu, T. Sakai, A. Sakamoto, Performance of lithium-ion battery with tin-phosphate glass anode and its characteristics, J. Electrochem. Soc. 160 (2013) A1725–A1730.
[91] C. Gejke, L. Borjesson, K. Edstrom, Cycling performance and temperature stability of a tin-borate glass anode, Electrochem. Commun. 5 (2003) 27–31.
[92] M.A. Kebede, N. Palaniyandy, R.M. Ramadan, E. Sheha, The electrical and electrochemical properties of graphene nanoplatelets modified 75V(2)O(5)-25P(2)O(5) glass as a promising anode material for lithium ion battery, J. Alloys Compd. 735 (2018) 445–453.
[93] J.D. Esper, F. Maussner, S. Romeis, Y. Zhuo, M.K.S. Barr, T. Yokosawa, E. Spiecker, J. Bachmann, W. Peukert, SiO_2-GeO_2 glass-ceramic flakes as an anode material for high-performance lithium-ion batteries, Energy Technol. (2022) 10.
[94] T. Chen, R. Li, J. Liu, D. Mu, S. Sun, L. Zhao, S. Tian, W. Zhu, X. Wang, C. Dai, Tin-based anode material with good reversibility of conversion reaction for lithium ion battery, J. Electroanal. Chem 880 (2021).
[95] B. Huang, Z. Pan, X. Su, L. An, Tin-based materials as versatile anodes for alkali (earth)-ion batteries, J. Power Sources 395 (2018) 41–59.
[96] X. Wu, X. Lan, R. Hu, Y. Yao, Y. Yu, M. Zhu, Tin-based anode materials for stable sodium storage: progress and perspective, Adv. Mater. 34 (2022).
[97] A.A. Ambalkar, U.V. Kawade, Y.A. Sethi, S.C. Kanade, M.V. Kulkarni, P. V. Adhyapak, B.B. Kale, A nanostructured SnO_2/Ni/CNT composite as an anode for Li ion batteries, RSC Adv. 11 (2021) 19531–19540.
[98] D. Liu, L. Wang, Y. He, L. Liu, Z. Yang, B. Wang, Q. Xia, Q. Hu, A. Zhou, Enhanced reversible capacity and cyclic performance of lithium-ion batteries using SnO_2 interpenetrated MXene V2C architecture as anode materials, Energy Technol. (2021) 9.
[99] N. Kuganathan, A. Kordatos, A. Chroneos, Li_2SnO_3 as a cathode material for lithium-ion batteries: defects, lithium ion diffusion and dopants, Sci. Rep. 8 (2018).
[100] A. Abouimrane, Y. Cui, Z. Chen, I. Belharouak, H.B. Yahia, H. Wu, R. Assary, L. A. Curtiss, K. Amine, Enabling high energy density Li-ion batteries through Li_2O activation, Nano Energy 27 (2016) 196–201.
[101] G. Kiran, G. Periyasamy, P.V. Kamath, Role of alloying in Cu_2O conversion anode for Li-ion batteries, Theor. Chem. Acc. 138 (2019) 1–10.
[102] Y. Wan, L. Wang, Y. Chen, X. Xu, Y. Wang, C. Teng, D. Zhou, Z. Chen, A high-performance tin dioxide@carbon anode with a super high initial coulombic efficiency via a primary cell prelithiation process, J. Alloys Compd. 740 (2018) 830–835.
[103] R. Fu, Y. Wu, C. Fan, Z. Long, G. Shao, Z. Liu, Reactivating Li_2O with nano-Sn to achieve ultrahigh initial coulombic efficiency SiO anodes for Li-ion batteries, ChemSusChem 12 (2019) 3377–3382.
[104] A.S. Kumar, M. Srinivas, A.P. Kiran, L. Neelakantan, Structural and electrochemical properties of (SnxCo100-x) 50C50 anodes for Li-ion batteries, Mater. Chem. Phys. 236 (2019), 121782.
[105] Y. Idota, T. Kubota, A. Matsufuji, Y. Maekawa, T. Miyasaka, Tin-based amorphous oxide: a high-capacity lithium-ion-storage material, Science 276 (1997) 1395–1397.
[106] B. Das, M.V. Reddy, B.V.R. Chowdari, SnO and SnO center dot CoO nanocomposite as high capacity anode materials for lithium ion batteries, Mater. Res. Bull. 74 (2016) 291–298.
[107] L. Liao, W. Huang, F. Cai, Q. Zhang, Preparation and mechanism of honeycomb-like nanoporous SnO_2 by anodization, J. Mater. Sci. Mater. Electron. 32 (2021) 9540–9550.
[108] J.H. Shin, J.Y. Song, Electrochemical properties of Sn-decorated SnO nanobranches as an anode of Li-ion battery, Nano Converg. (2016) 3.
[109] Y. Zhang, Glass anodes for lithium ion batteries: insight from the structural evolution during discharging/charging, Int. J. Appl. Glass Sci. 11 (2020) 577–589.
[110] J.Y. Lee, Y.W. Xiao, Z.L. Liu, Amorphous $Sn_2P_2O_7$, $Sn_2B_2O_5$ and Sn_2BPO_6 anodes for lithium ion batteries, Solid State Ionics 133 (2000) 25–35.
[111] M.N. Garaga, U. Werner-Zwanziger, J.W. Zwanziger, A. DeCeanne, B. Hauke, K. Bozer, S. Feller, Short-range structure of TeO_2 glass, J. Phys. Chem. C 121 (2017) 28117–28124.
[112] M. Levy, M. Duclot, F. Rousseau, V_2O_5-based glasses as cathodes for lithium batteries, J. Power Sources 26 (1989) 381–388.
[113] F. Kong, X. Liang, Y. Rao, X. Bi, R. Bai, X. Yu, Z. Chen, H. Jiang, C. Li, Glass anode crystallization for high specific capacity Lithium-ion batteries, Chem. Eng. J. (2022) 442.
[114] M. Seshasayee, K. Muruganandam, Molecular dynamics study of V_2O_5 glass, Solid State Commun 105 (1998) 243–246.
[115] K. Sharma, G.P. Kothiyal, L. Montagne, F.O. Mear, B. Revel, Synergic effect of V_2O_5 and P_2O_5 on the sealing properties of barium-strontium alumino-silicate glass/glass-ceramics, Int. J. Hydrogen Energy 38 (2013) 15542–15552.
[116] Y. Sakurai, J. Yamaki, V/sub 2/O/sub5/-P/sub 2/O/sub 5/glasses as cathode for lithium secondary battery, J. Electrochem. Soc. (United States) (1985) 132.
[117] Q. Xie, H. Ou, Q. Yang, X. Lin, A. Zeb, K. Li, X. Chen, G. Ma, A review on metal-organic framework-derived anode materials for potassium-ion batteries, Dalton Trans. 50 (2021) 9669–9684.
[118] Y. Wang, H. Fin, Q. Ma, K. Mo, H. Mao, A. Feldhoff, X. Cao, Y. Li, F. Pan, Z. Jiang, A MOF glass membrane for gas separation, Angew. Chemie-Int. Ed. 59 (2020) 4365–4369.
[119] C. Gao, Z. Jiang, S. Qi, P. Wang, L.R. Jensen, M. Johansen, C.K. Christensen, Y. Zhang, D.B. Ravnsbaek, Y. Yue, Metal-organic framework glass anode with an exceptional cycling-induced capacity enhancement for lithium-ion batteries, Adv. Mater. (2021).
[120] Y.I. Lee, J.H. Lee, S.H. Hong, Y.S. Park, Li-ion conductivity in Li_2O-B_2O_3-V_2O_5 glass system, Solid State Ionics 175 (2004) 687–690.
[121] S. Afyon, F. Krumeich, C. Mensing, A. Borgschulte, R. Nesper, New high capacity cathode materials for rechargeable li-ion batteries: vanadate-borate glasses, Sci. Rep. (2014) 4.
[122] Y. Chen, Y. Zhao, F. Liu, M. Ding, J. Wang, J. Jiang, P. Boulet, M.C. Record, Structural and electrochemical properties of Li_2O-V_2O_5-B_2O_3-Bi_2O_3 glass and glass-ceramic cathodes for lithium-ion batteries, Molecules 28 (2023) 229.
[123] A. Hayashi, Characterization of Li_2S–SiS_2–Li_3MO_3 (M=B, Al, Ga and In) oxysulfide glasses and their application to solid state lithium secondary batteries, Solid State Ionics 152-153 (2002) 285–290.
[124] S. Kondo, K. Takada, Y. Yamamura, New lithium ion conductors based on Li_2S-SiS_2 system, Solid State Ionics 53-56 (1992) 1183–1186.
[125] H. Morimoto, H. Yamashita, M. Tatsumisago, T. Minami, Mechanochemical Synthesis of the High Lithium Ion Conductive Amorphous Materials in the Systems Li_2S-SiS_2 and Li_2S-SiS_2-Li_4SiO_4, J. Ceramic Soc. Jpn. 108 (2000) 128–131.
[126] K. Itoh, M. Sonobe, K. Mori, M. Sugiyama, T. Fukunaga, Structural observation of Li_2S–GeS_2 superionic glasses, Phys. B Condensed Matter 385-386 (2006) 520–522.
[127] R. Kanno, Synthesis of a new lithium ionic conductor, thio-LISICON–lithium germanium sulfide system, Solid State Ionics 130 (2000) 97–104.
[128] S. Ujiie, A. Hayashi, M. Tatsumisago, Structure, ionic conductivity and electrochemical stability of Li_2S–P_2S_5–LiI glass and glass–ceramic electrolytes, Solid State Ionics 211 (2012) 42–45.
[129] Y. Zhang, K. Chen, Y. Shen, Y. Lin, C.W. Nan, Synergistic effect of processing and composition x on conductivity of xLi_2S-$(100-x)P_2S_5$ electrolytes, Solid State Ionics 305 (2017) 1–6.
[130] F. Mizuno, All-solid-state lithium secondary batteries using Li_2S-SiS_2-Li_4SiO_4 glasses and Li_2S-P_2S_5 glass ceramics as solid electrolytes, Solid State Ionics 175 (2004) 699–702.
[131] M. Tatsumisago, A. Hayashi, Superionic glasses and glass–ceramics in the Li_2S–P_2S_5 system for all-solid-state lithium secondary batteries, Solid State Ionics 225 (2012) 342–345.
[132] K. Mori, K. Iwase, Y. Oba, K. Ikeda, T. Otomo, T. Fukunaga, Structural and electrochemical features of $(Li_2S)(x)(SiS_2)(100-x)$ superionic glasses, Solid State Ionics 344 (2020), 115141.
[133] H. Tsukasaki, S. Mori, S. Shiotani, H. Yamamura, Ionic conductivity and crystallization process in the Li_2S–P_2S_5 glass electrolyte, Solid State Ionics (2018).
[134] H. Tsukasaki, H. Morimoto, S. Mori, Ionic conductivity and thermal stability of Li_2O–Li_2S–P_2S_5 oxysulfide glass, Solid State Ionics 347 (2020), 115276.
[135] T. Ohtomo, F. Mizuno, A. Hayashi, K. Tadanaga, M. Tatsumisago, Electrical and electrochemical properties of Li_2S–P_2S_5–P_2O_5 glass–ceramic electrolytes, J. Power Sources 146 (2005) 715–718.
[136] A. Hayashi, H. Muramatsu, T. Ohtomo, S. Hama, M. Tatsumisago, Improved chemical stability and cyclability in Li_2S–P_2S_5–P_2O_5–ZnO composite electrolytes for all-solid-state rechargeable lithium batteries, J Alloys Compd. 591 (2014) 247–250.
[137] A. Yamauchi, A. Sakuda, A. Hayashi, M. Tatsumisago, Preparation and ionic conductivities of $(100-x)(0.75Li_2S{\cdot}0.25P_2S_5){\cdot}xLiBH_4$ glass electrolytes, J. Power Sources 244 (2013) 707–710.
[138] S. Ujiie, A. Hayashi, M. Tatsumisago, Preparation and ionic conductivity of $(100-x)(0.8Li_2S{\cdot}0.2P_2S_5)\cdot$ xLiI glass–ceramic electrolytes, J. Solid State Electrochem. 17 (2012) 675–680.
[139] A. Kato, M. Yamamoto, A. Sakuda, A. Hayashi, M. Tatsumisago, Mechanical Properties of Li_2S–P_2S_5 Glasses with Lithium Halides and Application in All-Solid-State Batteries, ACS Appl. Energy Mater. (2018) 1002–1007.
[140] A. Hayashi, S. Hama, T. Minami, M. Tatsumisago, Formation of superionic crystals from mechanically milled Li_2S–P2S5 glasses, Electrochem. Commun. 5 (2003) 111–114.
[141] Y. Zhang, R. Chen, T. Liu, Y. Shen, Y. Lin, C.W. Nan, High Capacity, Superior cyclic performances in all-solid-state lithium-ion batteries based on $78Li_2S$-$22P_2S_5$ glass-ceramic electrolytes prepared via simple heat treatment, ACS Appl. Mater Interfaces 9 (2017) 28542–28548.
[142] F. Mizuno, A. Hayashi, K. Tadanaga, M. Tatsumisago, New, Highly Ion-Conductive Crystals Precipitated from Li2S-P2S5 Glasses, Adv. Mater. 17 (2005) 918–921.
[143] H. Nagata, J. Akimoto, All-oxide solid-state lithium-ion battery employing $50Li_2SO_4$–$50Li_2CO_3$ glass electrolyte, J. Power Sources 491 (2021), 229620.
[144] C. Lee, Characterizations of a new lithium ion conducting Li_2O–SeO_2–B_2O_3 glass electrolyte, Solid State Ionics 149 (2002) 59–65.
[145] A. Hayashi, Thermal and electrical properties of rapidly quenched Li_2S-SiS_2-Li_2O-P_2O_5 oxysulfide glasses, Solid State Ionics 113–115 (1998) 733–738.